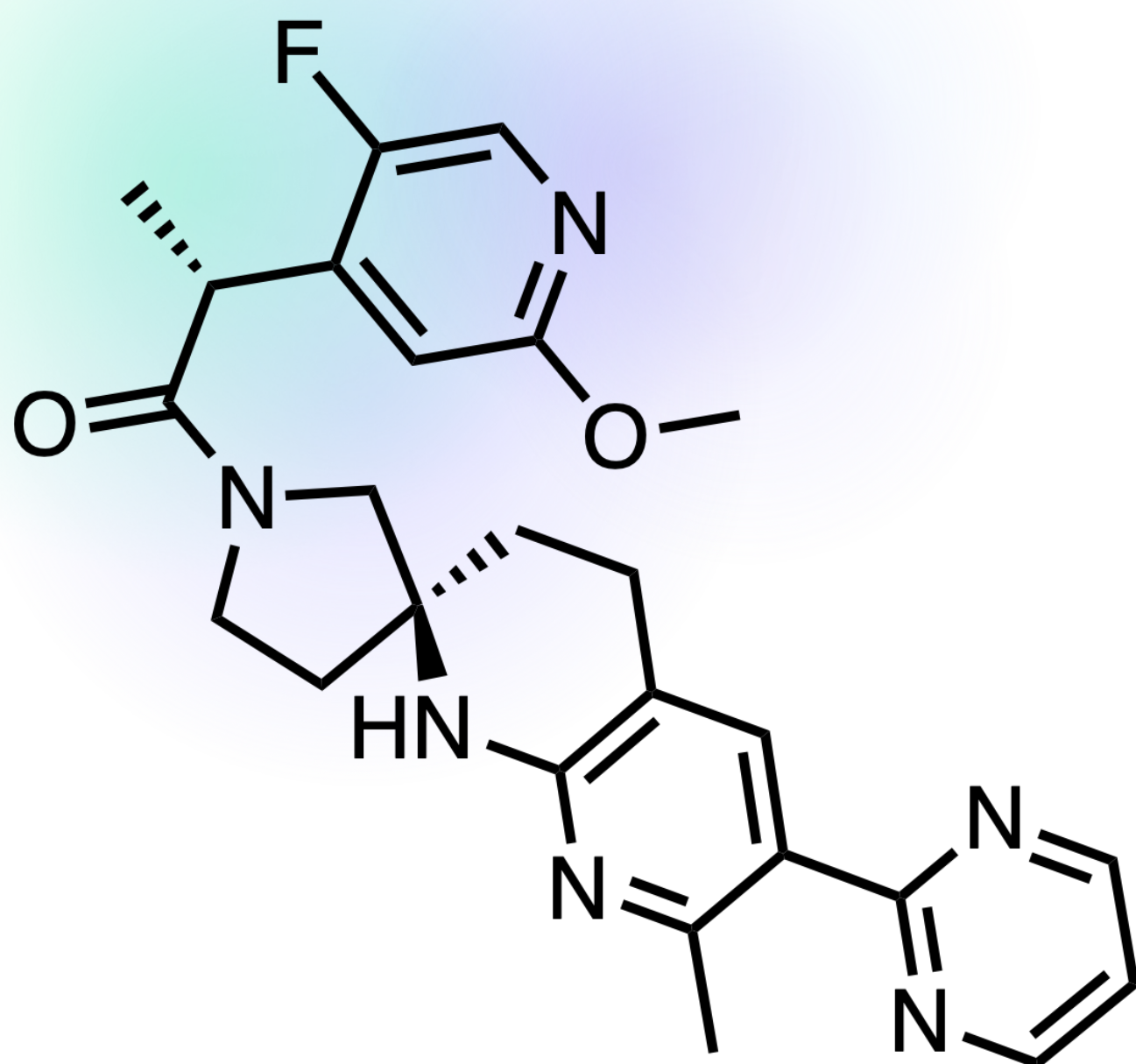


drughunter.com

Small Molecules of the Month

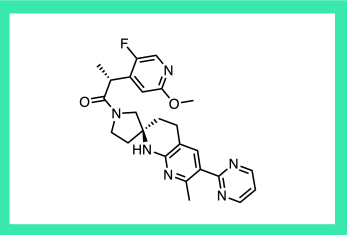
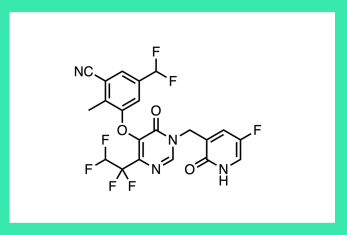
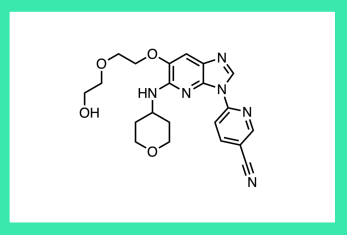
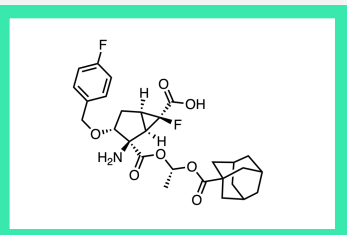
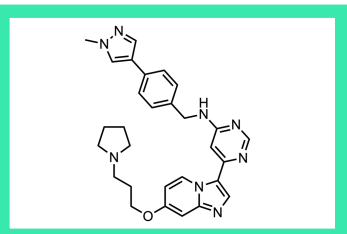
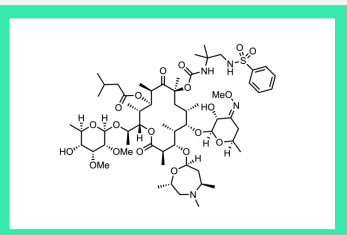
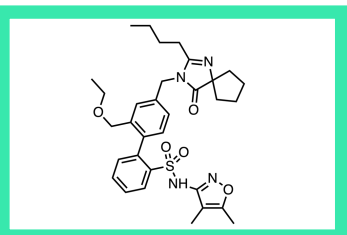
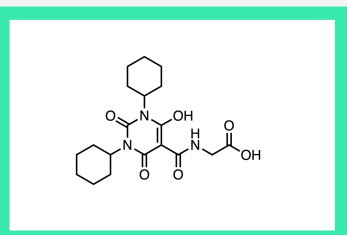
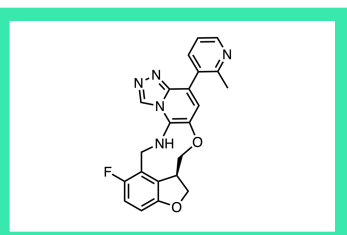
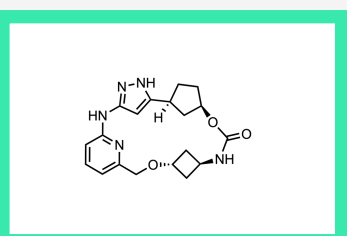
February 2023



drug
hunter

Table of Contents

February 2023

Page 3	PF-07258669 MCR4	oral melanocortin-4 receptor antagonist	Ph. I candidate	PFIZER INC., GROTON, CT	
Page 6	PYR01 HIV Gag-Pol	bifunctional, Gag-Pol allosteric glue	NNRTI + nanomolar ex vivo HIV-1 TACK activity	MERCK & CO. INC., RAHWAY, NJ	
Page 8	GLPG2534 IRAK4	oral IRAK4 inhibitor	promising activity in mouse model for atopic dermatitis	GALAPAGOS, FR + BE	
Page 10	TPO473292 mGluR2/3	mGluR2/3 antagonist prodrug	Ph. II for depression	TAISHO PHARMACEUTICAL CO., TOKYO, JP	
Page 13	M4205 KIT	selective KIT inhibitor	Ph I. for advanced GIST	MERCK HEALTHCARE KGAA, DARMSTADT, DE	
Page 16	SEQ-9 Mtb 23S ribosome	oral Mtb 23S bacterial ribosome inhibitor	potent in vitro + in vivo activity against <i>Mycobacterium tuberculosis</i>	SANOVI, FR + CH	
Page 18	sparsentan ET/ATR	FIC oral, once-daily, dual ET _A /AT ₁ antagonist	FDA-approved for proteinuria reduction in primary IgAN	TRAVERE THERAPEUTICS, SAN DIEGO, CA	
Page 20	daprodustat HIF-PHD	oral, once-daily, pan-PHD inhibitor	FDA-approved for anemia in CKD patients	GSK, PLC, LONDON, UK	
Page 22	pociredir EED (PRC2)	oral, allosteric PRC2 inhibitor (EED)	Ph. IIb for sickle cell disease (on hold)	FULCRUM THERAPEUTICS, MA	
Page 25	QR-6401 CDK2	oral, macrocyclic CDK2 inhibitor	robust activity in ovarian cancer xenograft models	REGOR THERAPEUTICS GROUP, SHANGHAI, CN	

February 2023

PF-07258669

MCR4

oral melanocortin-4 receptor antagonist

Ph.I candidate

focused screen of 28K library for MC4R activity

J. Med. Chem., February 19, 2023

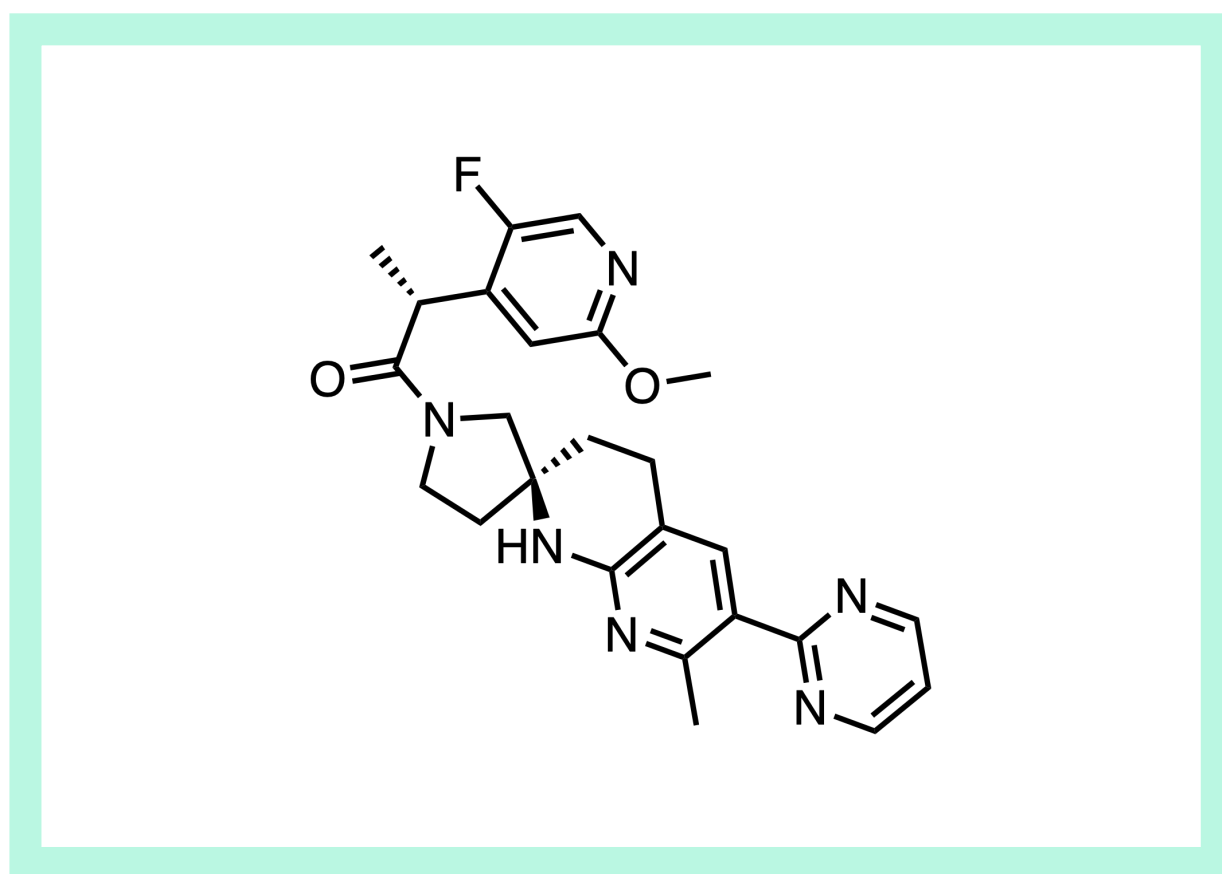
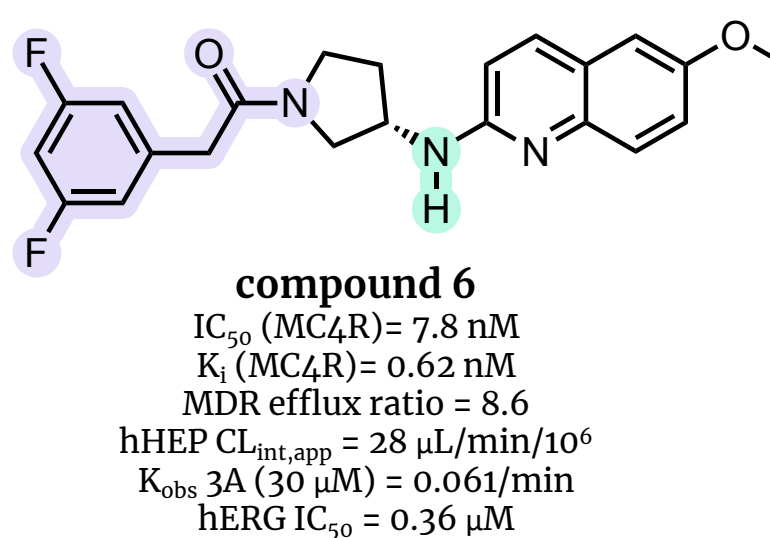
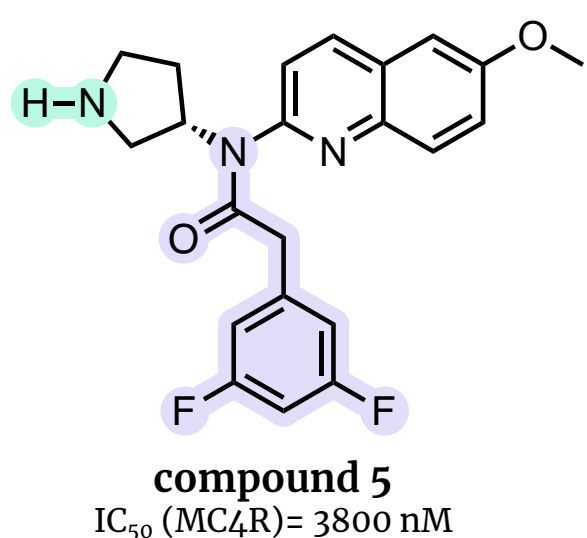
PFIZER INC., GROTON, CT

paper DOI: <https://doi.org/10.1021/acs.jmedchem.2c02012>

[View Online](#)

MC4R antagonism to help gain weight. PF-07258669 is a [melanocortin-4 receptor \(MC4R\)](#) antagonist intended to help increase weight gain, in contrast to MC4R agonists which have been studied extensively in the industry for weight loss. The peptidic MC4R agonist, [setmelanotide](#), for example, was approved in 2020 for the treatment of obesity. An MC4R antagonist like PF-07258669 could instead be helpful for treating [cachexia](#), a metabolic disorder that results in weight and muscle loss associated with advanced cancer and the late stages of other major chronic illnesses. It has been [estimated](#) to affect 9 million patients in the industrialized world, including 50-80% of cancer patients. The standard of care according to [current clinical guidelines](#) includes dietary counseling, oral nutritional supplements, and pharmacological interventions such as progesterone analogs and corticosteroids. A [variety of therapeutic approaches](#) have been investigated but cachexia remains a significant unmet medical need.

The first MC4R antagonist to enter clinical trials. The [melanocortin-4 receptor](#) is a G-protein-coupled receptor that is regulated by endogenous peptide agonists and antagonists in response to nutritional state and plays an important role in energy homeostasis. MC4R antagonists increase food intake and reduce weight loss in animal models of cachexia ([mice](#), [mice](#), [mice](#), [dogs](#)). MC4R homozygous [knockout mice](#) develop a maturity-onset obesity syndrome characterized by hyperphagia, hyperinsulinemia, and hyperglycemia. A number of MC4R antagonists have been reported to have activity in pre-clinical models of cachexia, including [ML00253764](#), [TCMCB07](#), [BL-6020/979](#), [SNT207707](#), and [SNT209858](#), though few structures have been disclosed. PF-07258669 is the first disclosed MC4R antagonist to enter clinical trials.



An initially misassigned, rearranged **antagonist** hit from a focused screen of MC4R **agonist** ligands. Focused screening campaigns for identifying MC4R agonists had been carried out previously on a 28K compound library at Pfizer. For this particular campaign, this data was then mined for compounds that displayed MC4R affinity, plus possible antagonist or inverse agonist activity, followed by a functional MC4R inverse agonist assay for confirmation. This led to the identification of a micromolar starting point “compound 5” (IC₅₀ = 3.8 μM), which exhibited agonist activity that happened to improve over time. Upon deeper investigation, it was revealed that the 3-acyl aminopyrrolidine could undergo an acyl migration to the 1-acyl aminopyrrolidine of “compound 6.” This rearranged compound demonstrated high affinity for MC4R (K_i = 0.62 nM) and nanomolar antagonist activity (IC₅₀ = 7.8 nM). Despite the impressive MC4R affinity and potency of “compound 6,” it was also a potent hERG inhibitor (IC₅₀ = 0.36 μM) and displayed time-dependent CYP450 3A₄ inhibition (K_{obs} 3A, 30 μM = 0.061/min).

Strategies for improving potency, safety and PK properties. Substitution of the methoxy quinoline with a pyridyl triazole resulted in a drop in potency and high efflux, but better metabolic stability in hepatocytes. Addition of a CF₃ to the triazole helped improve that MDR efflux ratio. Exploring the *p*-fluorophenyl SAR led to a methoxypyridine replacement with improved lipophilicity (logD = 2.1) and hHEP turnover (clearance). Introduction of the methyl group adjacent to the amide significantly improved MC4R potency, while addition of a F-substituent to the pyridine ring further improved MDR efflux. However, metabolic profiling revealed *N*-desmethyl analogs that reintroduced cardiac and metabolic liabilities, which could not be otherwise mitigated by deuterium incorporation or [4.4]- or [4.5]- (hetero)spirocycle replacements.

February 2023

PF-07258669

MCR4

oral melanocortin-4 receptor antagonist

Ph.I candidate

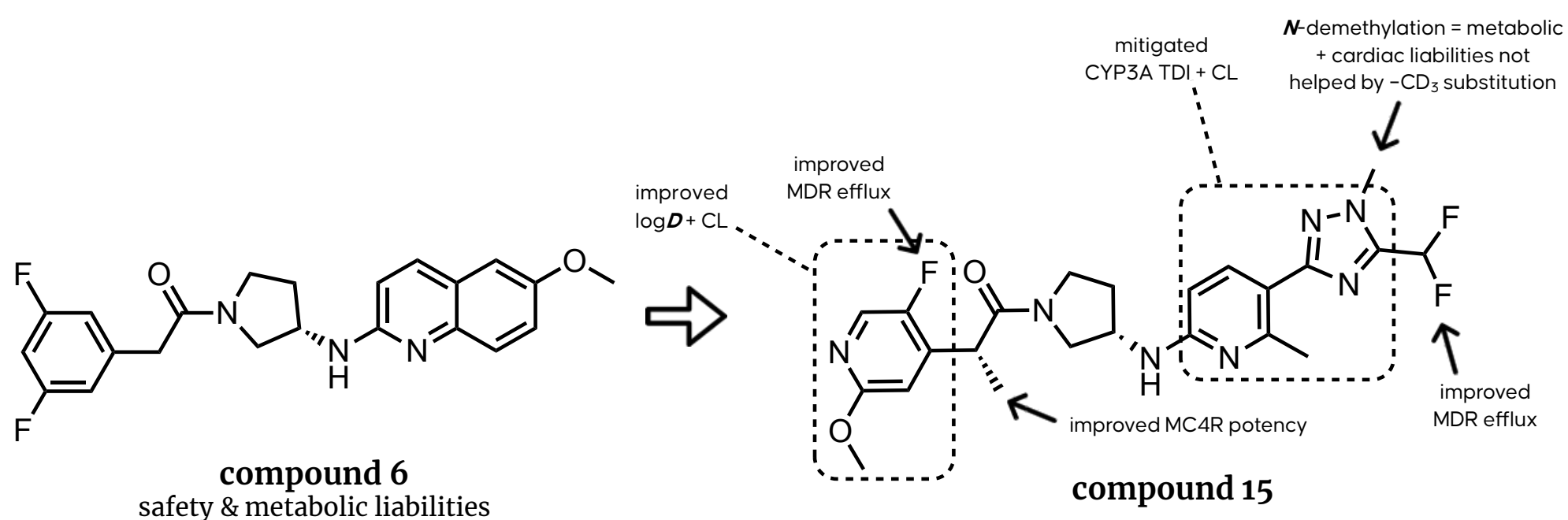
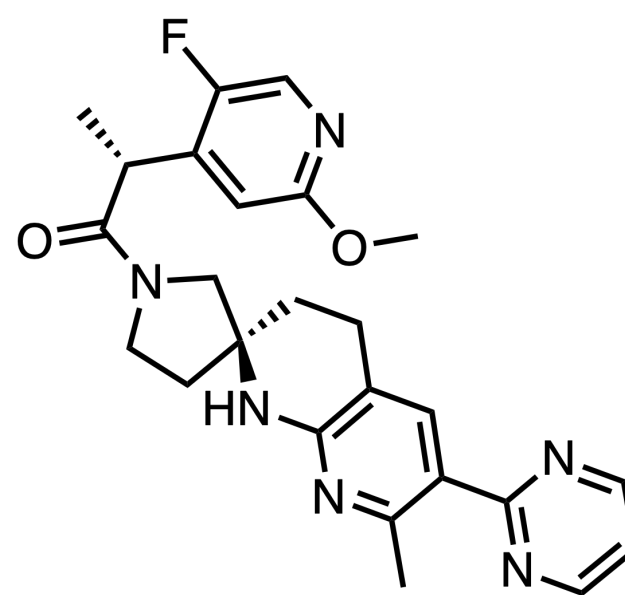
focused screen of 28K library for MC4R activity

J. Med. Chem., February 19, 2023

PFIZER INC., GROTON, CT

paper DOI: <https://doi.org/10.1021/acs.jmedchem.2c02012>

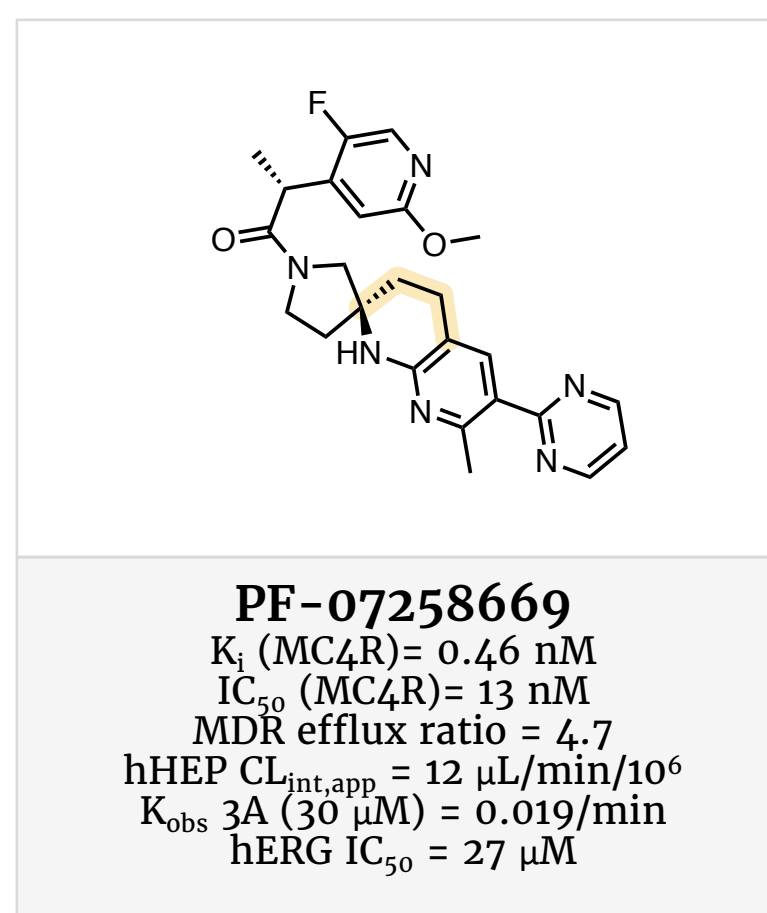
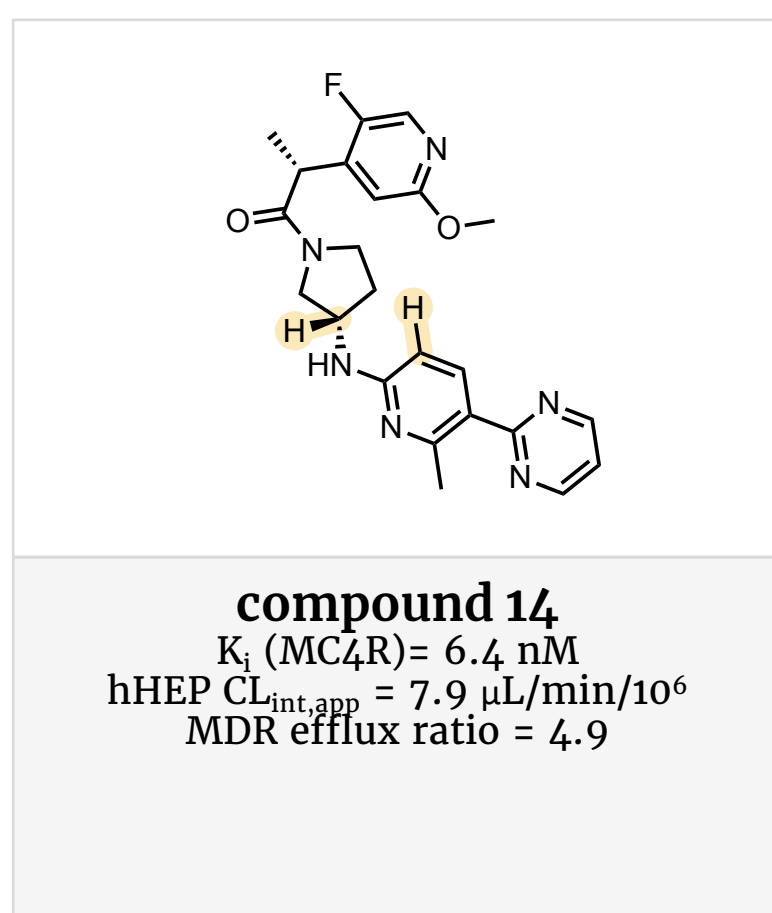
[View Online](#)



Spirocyclization increases potency through restriction to a bioactive conformation. During optimization, calculations based on published X-ray crystal structures and NMR residual dipolar coupling (RDC) studies revealed that the aminopyridine preferred an inactive, *trans*-conformation, resulting in suboptimal potency. Spirocyclization was used to lock the orientation of the ring system in the desired *cis*-bioactive conformation. This approach was supported by the [small molecule x-ray crystal structure of 6](#) and NMR studies of its conformation in solution. Switching from the 5-membered N-heterocycle to a pyrimidine moiety with a [4.5]-diazaspirocycle resulted in

the Ph. I candidate, “compound 23.” Comparison of the linear “compound 14” to its spirocyclic counterpart, PF-07258669, resulted in a 14-fold improvement in potency ($K_i = 6.4$ nM vs. $K_i = 0.46$ nM).

Binding mode of MC4R antagonists. Although a structure for the binding of PF-07258669 to MC4R hasn't been reported, an [x-ray crystal structure](#) of MC4R bound to a peptide antagonist is available (PDB: [6W25](#)). The [cryo-EM structure](#) of MC4R bound to setmelanotide (a peptide agonist recently approved for obesity) has also been reported (PDB: [7AUE](#)).



February 2023

PF-07258669

MCR4

oral melanocortin-4 receptor antagonist

Ph.I candidate

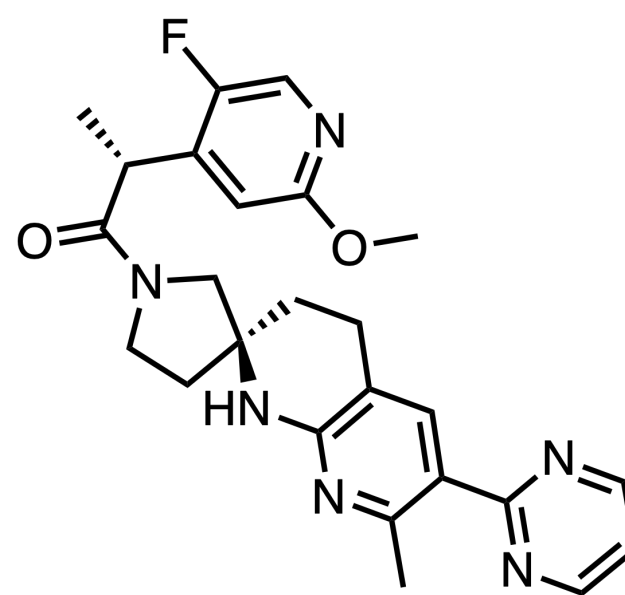
focused screen of 28K library for MC4R activity

J. Med. Chem., February 19, 2023

PFIZER INC., GROTON, CT

paper DOI: <https://doi.org/10.1021/acs.jmedchem.2c02012>

[View Online](#)



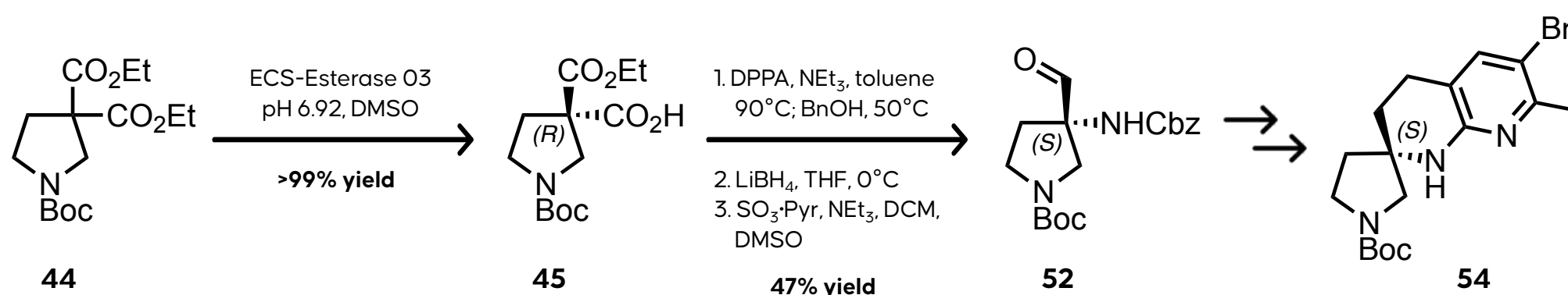
Preclinical pharmacology. PF-07258669 had good selectivity against several other hMCR subtypes (hMC1R $K_i > 1600$ nM, hMC3R $K_i = 340$ nM, hMC5R $K_i = 840$ nM). Off-target screening against a panel of 105 targets at 10 μ M showed that all had <50% response. The compound displayed a good PK profile in rats (CL = 21 mL/min/kg, $V_{ss} = 0.95$ L/kg, $t_{1/2} = 1$ h, %F = 28) and dogs (CL = 11 mL/min/kg, $V_{ss} = 1.3$ L/kg, $t_{1/2} = 2.3$ h, %F = 93). The brain penetration ratio was also studied in rats (total brain-to-plasma ratio = 0.23, brain-to-unbound plasma ratio = 0.1). In an aged rat model of geriatric anorexia, twice-daily (BID) administration of the compound resulted in dose-dependent increases in food intake and body weight. There were no safety issues with 14-day dosing in Wistar Han rats or 8-day dosing in beagle dogs (dose amount not disclosed).

Clinical development. PF-07258669 was studied in a Phase I clinical trial ([NCT04628793](#), n = 29) and a second Phase I trial is underway ([NCT05113940](#),

n = 150, estimated completion date 4/14/23). Participants in this study will receive either standard, high fat/high calorie, or high carbohydrate/high calorie diets. An optional cohort in Part A may include healthy Japanese adults; Part B of the trial will evaluate the effect of PF-07258669 on midazolam PK in healthy adult participants.

Synthesis highlight: an enzyme-catalyzed desymmetrization key step. The chiral stereocenter of **45** was installed via an enzyme-catalyzed desymmetrization of achiral diester **44** with ECS-Esterase 03. This was followed by Curtius rearrangement to the Cbz-amine, transformation of the other ester to the aldehyde, followed by a few more manipulations including an intramolecular cyclization under Buchwald coupling conditions to afford spirocycle **54**.

Patents: "Spiro compounds as melanocortin 4 receptor antagonists and uses thereof": [WO2021250541A1](#) (2021)



February 2023

PYR01

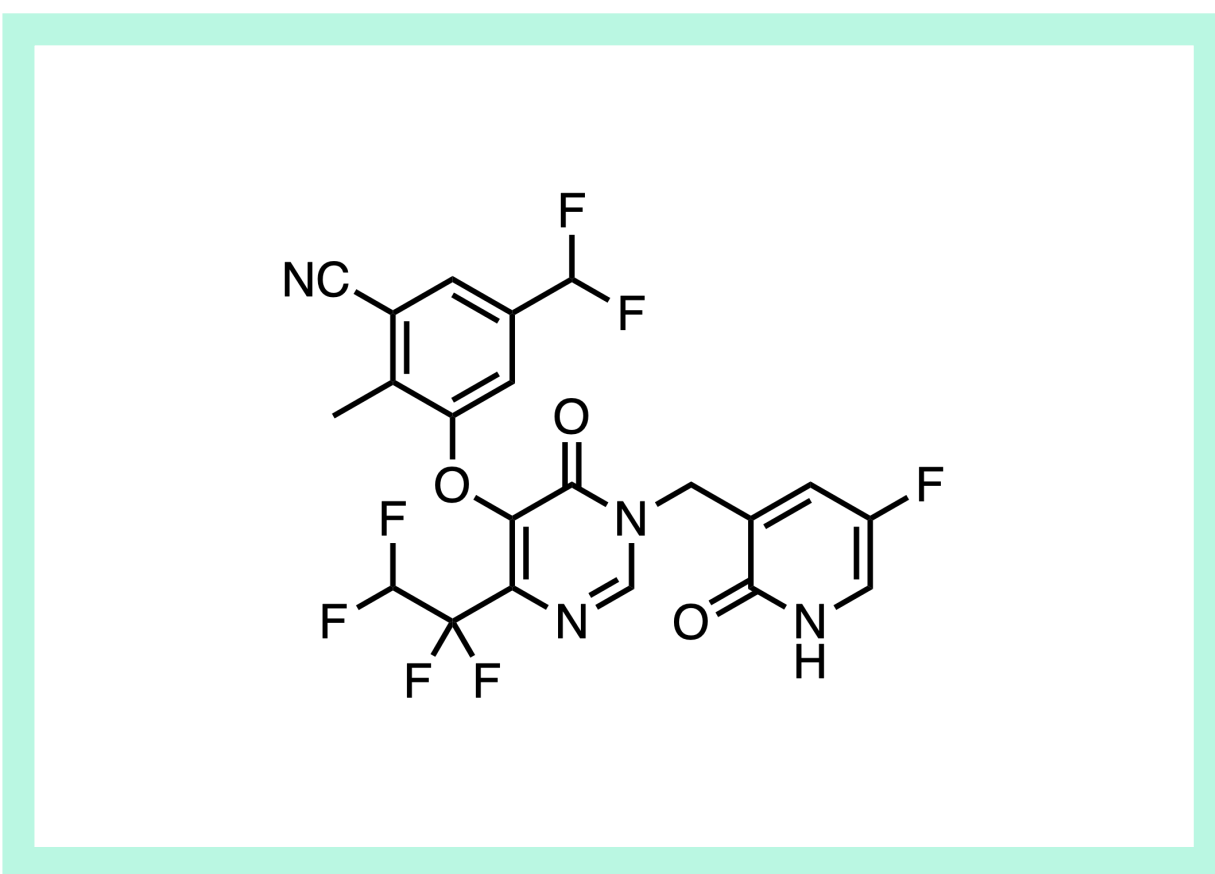
HIV Gag-Pol

bifunctional, Gag-Pol allosteric glue
NNRTI + nanomolar ex vivo HIV-1 TACK activity
HTS of >6K NNRTIs for TACK activity
Sci. Transl. Med., February 22, 2023
MERCK & CO. INC., RAHWAY, NJ
paper DOI: <https://doi.org/10.1126/scitranslmed.abn2038>

[View Online](#)

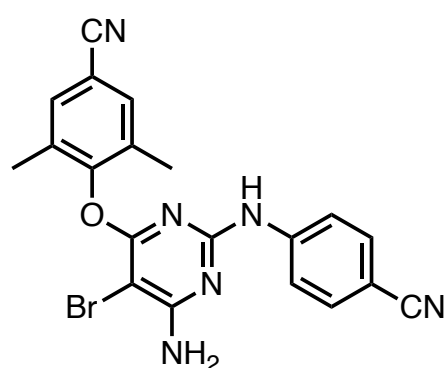
Harnessing a novel mechanism for HIV eradication with a new class of bifunctional molecules. Modern antiretroviral therapies (ARTs) efficiently block HIV-1 replication, but are not completely curative because they can't deplete viral reservoirs hidden from the immune system within the host genome. **PYR01** is an HIV antiviral which, unlike traditional HIV drugs, is able to selectively kill HIV-1-infected cells that serve as cure-preventing viral reservoirs, in addition to the early-stage antiviral activity. This non-nucleoside reverse transcriptase inhibitor (NNRTI) is able to accomplish this through optimized potency for a secondary allosteric glue function that promotes dimerization of reverse transcriptase (RT), premature intracellular HIV-1 protease activation, cleavage and activation of host proteins including the CARD8 inflammasome, ultimately leading to pyroptotic cell death. The molecule is able to kill HIV-1-infected CD4+ T-cells from HIV-1 patients, providing ex vivo proof-of-concept for this new approach to HIV clearance.

A hidden secondary activity within existing NNRTIs. There are currently 5 approved NNRTIs: etravirine (ETR, INTELENCE), nevirapine (NVP, VIRAMUNE), rilpivirine (RPV, EDURANT), efavirenz (EFV, SUSTEVA), and

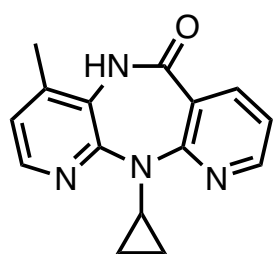


doravirine (DOR, PIFELTRO); as well as various approved combination therapies. NNRTIs normally target the early stages of infection by allosterically inhibiting RT-catalyzed translation of viral RNA into double-stranded DNA. However, it has been known since the 2000's that some NNRTIs, like efavirenz, demonstrated additional late-stage antiviral activity that could result in HIV-1-infected cell-killing. However, molecules like efavirenz had significantly reduced potency for this secondary cell-killing activity relative to their antiviral activity, making this cell-killing function clinically irrelevant.

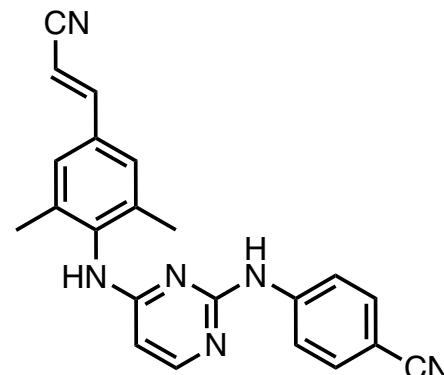
A phenotypic screen for NNRTIs with cell-kill activity. Merck scientists saw promise in the secondary targeted activation of cell-kill (TACK) activity of certain NNRTIs and wondered if it could be made clinically actionable through molecules with improved cell-kill potency. A subset of 6628 NNRTIs were screened in a phenotypic assay measuring the ability to selectively terminate HIV-1+ cells, using PBMCs infected with GFP-expressing HIV-1 virus. TACK activity was rare among the NNRTIs tested, but a pyrimidone series related to doravirine showed promise, and was the focus of optimization.



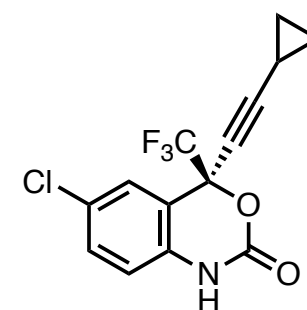
etravirine
(ETR, INTELENCE®)



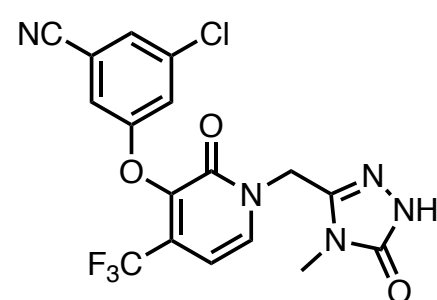
nevirapine
(NVP, VIRAMUNE®)



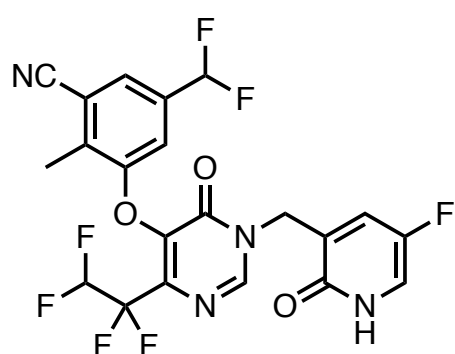
rilpivirine
(RPV, EDURANT®)



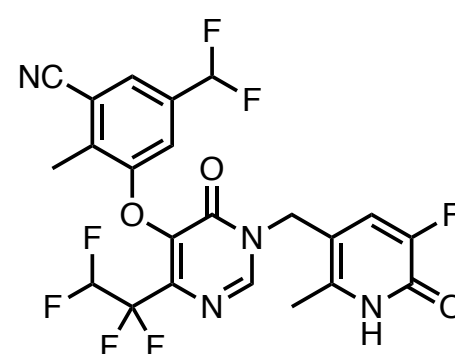
efavirenz
(EFV, SUSTEVA®)



doravirine
(DOR, PIFELTRO®)



PYR01



PYR02

February 2023

PYR01

HIV Gag-Pol

bifunctional, Gag-Pol allosteric glue

NNRTI + nanomolar ex vivo HIV-1 TACK activity

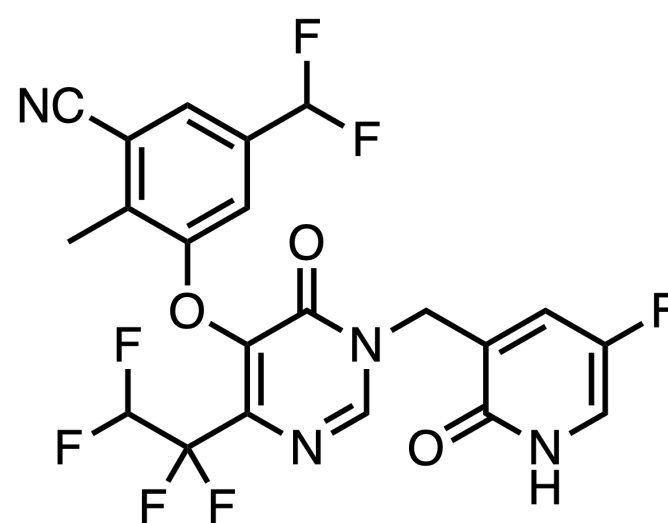
HTS of >6K NNRTIs for TACK activity

Sci. Transl. Med., February 22, 2023

MERCK & CO. INC., RAHWAY, NJ

paper DOI: <https://doi.org/10.1126/scitranslmed.abn2038>

[View Online](#)



NNRTIs	PYR01	PYR02	doravirine	efavirenz	nevirapine
antiviral IC ₅₀	40 nM	131 nM	13 nM	34 nM	219 nM
TACK WT EC ₅₀ (HIV+ PBMC)	28 nM	34 μM	8.9 μM	1.6 μM	> 41 μM
RT dimerization WT EC ₅₀	24 nM	3.6 μM	-	210 nM	> 68 μM
TACK WT EC ₅₀ (HIV+ CD4 ⁺ T)	38 nM	> 41 μM	-	4.1 μM	> 41 μM
cytotoxicity CC ₅₀	> 40 μM	> 40 μM	> 40 μM	> 40 μM	> 40 μM

IC₅₀ = half-maximal inhibitory concentration values, measured in a std HIV-1 antiviral assay in HIV+ MT4-GFP cells, dimerization measured with HTRF with recombinant HIV-1 RT-p66 proteins (His- or FLAG-tagged), CC₅₀ = half-maximal cytotoxic concentration, assessed in uninfected PBMCs ± PHA stimulation + CD4⁺ T cells ± CD3/CD28 activation.

HIV+ cell-killing activity is not correlated to HIV antiviral activity or binding mode. PYR01 and 02 are structurally similar to each other (76% Tanimoto similarity score), differ by only two ring substitutions, and have similar antiviral activity, yet have cell-kill (TACK) activity that differs by orders of magnitude (28 nM for PYR01 vs. 34 μM for PYR02). This disconnect between antiviral activity and cell-kill activity is seen outside of this series as well, with PYR01 having much greater TACK potency than doravirine (8.9 μM) and structurally unrelated NNRTIs, nevirapine (NVP, > 41 μM) and efavirenz (EFV, 1.6 μM). X-ray crystal structure analysis with HIV-1 RT (p66/p51) heterodimer showed that PYR01 has two H-bonding interactions with its C-ring (PDB: [7SLR](#)), while PYR02 only has one (PDB: [7SLS](#)). The two H-bonding interactions of PYR01 induce a slight (1 Å) shift in the protein backbone, but doesn't affect the dimerization interface. The general binding conformations of the two compounds within the mature RT dimer are therefore quite similar, and determined not to be the cause of the discrepancy in TACK activity.

Instead, allosterically-driven RT dimerization strongly correlates to TACK activity. The ability of the compounds to induce dimerization of [RT-p66 subunit](#) was evaluated. PYR01 demonstrated an HIV1 RT-p66 dimerization EC₅₀ of 24 nM, an order of magnitude more potent than EFV (dimer EC₅₀ = 210 nM) and two orders more potent than PYR02 (dimer EC₅₀ = 3600 nM). Further studies showed that PYR01-induced RT dimerization occurred relatively quickly, reaching equilibrium within 18 hours. In contrast, PYR02 showed weak RT dimerization activity, with only ~10-fold potency improvement at day 9 ([from Table S1](#)). Additional radiolabeling studies supported the hypothesis that the allosteric (and not direct) binding of NNRTIs to monomeric RT-p66 was accelerating the rate of RT dimerization and inducing the HIV-1-infected cell cytotoxicity. Additional studies to assess antiviral activity in NNRTI-resistant HIV variants demonstrated that PYR01 generally

outperformed PYR02, EFV and NVP with 10-1000-fold higher potencies. Thus, this approach of screening and optimization focused on TACK activity rather than antiviral activity had the additional benefit of resulting in more potent antiviral agents for NNRTI-resistant strains.

“Real-world” proof-of-concept with activity in CD4⁺ T cells from people living with HIV/AIDS. In vitro studies performed with CD4⁺ T cells obtained from people living with HIV/AIDS (PLWH) on suppressive antivirals showed in vitro efficacy for PYR01. PYR01 and EFV in combination reduced Gag p24 production across 8 donors (97% and 92% in cell pellets + 94% and 85% in supernatants, respectively), but not for PYR02 + NVP. Even further, both PYR01 and EFV cleared the infected cells without negatively affecting the CD4⁺ T cell population. All of these preclinical results support PYR01 acting as a TACK and allosteric molecular glue, inducing the aforementioned cascade in latent infected cells of RT dimerization, premature HIV protease activity, and subsequent elimination of the HIV-infected cells, all independent of immune recognition.

What's next? While this study identified bifunctional NNRTIs with dually potent antiviral and HIV-1-infected cell kill properties, the latter has only been demonstrated in vitro, not yet in vivo. A potential hurdle for the TACK mechanism to overcome is that it [requires intact Gag-Pol expression and corresponding premature HIV-1 protease activation](#). Therefore, cells that are translationally silent or have inactive provirus may still not be affected by PYR01 or similar molecules, allowing a small reservoir of HIV to potentially remain. Experiments pairing TACK molecules with latency-reversal agents may provide more insight into a potential path forward toward HIV eradication. Overall, if molecules with a TACK activity are successful in the clinic, they could provide an additional option to address HIV treatment durability, overcome resistance, and ultimately play a role in a future curative regimen for HIV.

February 2023

GLPG2534

IRAK4

oral IRAK4 inhibitor

promising activity in mouse model for atopic dermatitis

HTS of kinase-focused 25K compd library vs. IRAK4 catalytic domain

Sci. Trans. Med., February 15, 2023

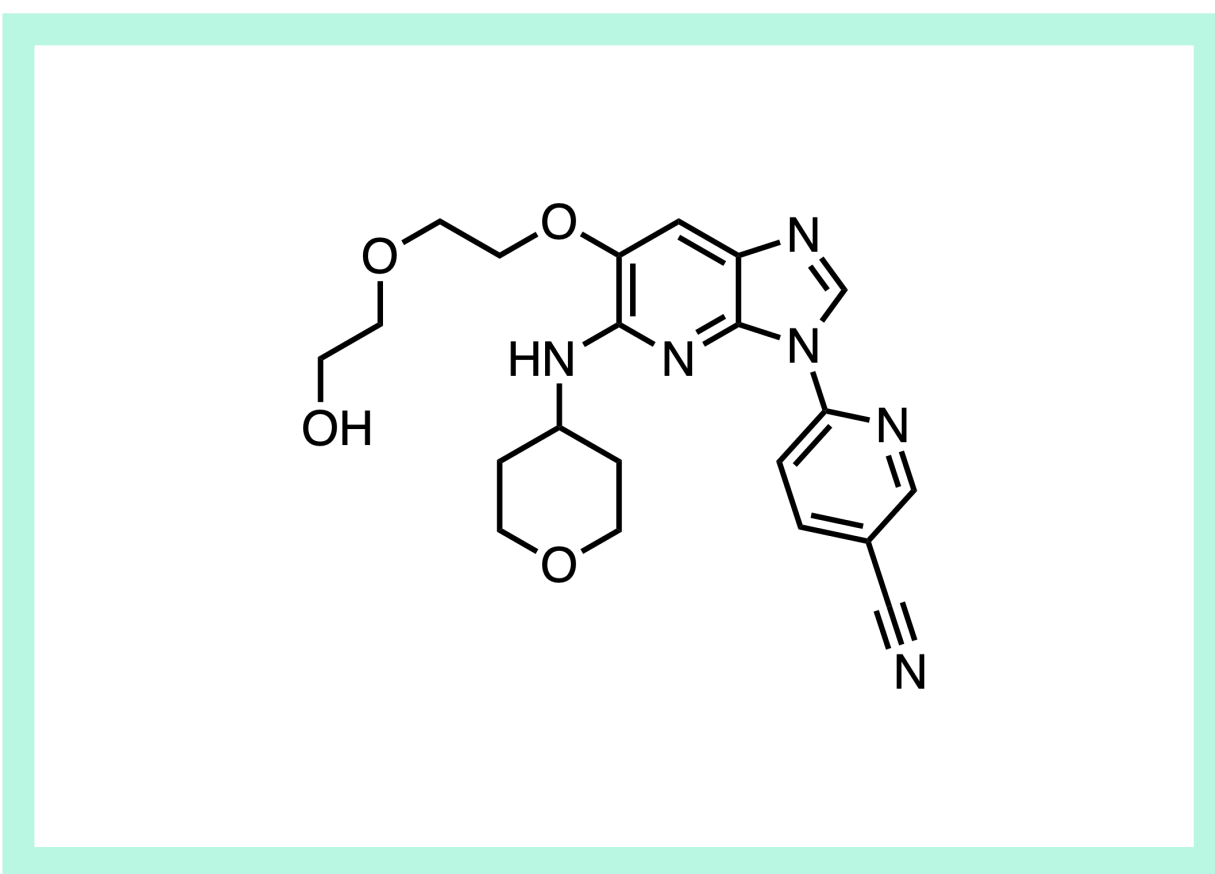
GALAPAGOS, FR + BE

paper DOI: <https://doi.org/10.1126/scitranslmed.abj3289>

[View Online](#)

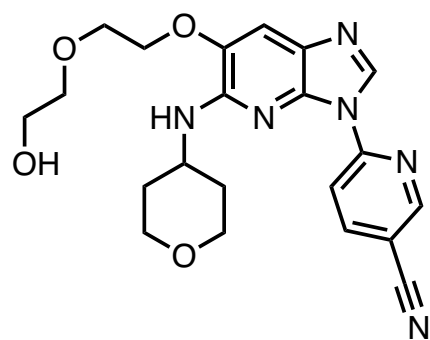
Preclinical validation for IRAK4 inhibitors for dermatology from activity in human biopsies. Interleukin-1 receptor-associated kinase ([IRAK4](#)) is downstream of toll-like receptors ([TLRs](#)), which are established [mediators of inflammation](#). Like many immune-signaling nodes (JAK, BTK), this has been of interest for potential treatment of [immunological diseases](#) and [blood cancers](#) with immune-cell lineages. Paralleling the development of [JAK inhibitors](#), IRAK4 biology was preclinically validated for RA and SLE initially, and now Galapagos is disclosing preclinical validation for dermatology, the ATP-competitive clinical candidate, GLPG2534. Particularly notable here is that [IRAK4 inhibition](#) with Galapagos' compound ameliorated pathogenic molecular signatures in biopsies of diseased human tissue.

IRAK4, the “JAK” or “BTK” of innate immunity? Given the massive success of molecules targeting T-cell receptor signaling mediators in the [JAK family](#) and B-cell receptor signaling mediator [BTK](#), it's no wonder IRAK4 has been a “hot” [target](#) given its role as a [key mediator of signaling](#) by toll-like receptors, key players in innate immunity. In inflammation, immuno-oncology (think [TLR7/8](#), [STING](#)) and hematology, modulators of innate immunity have not yet seen the



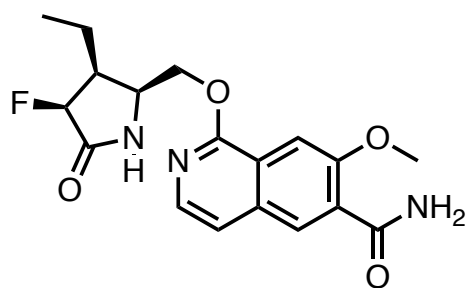
dramatic success of modulators of adaptive immunity (i.e., T-cell and B-cell biology), but research continues along many channels.

What's known about its discovery? Six hits (structures not disclosed) were found using a high throughput screen with a kinase-focused library of 25K compounds for competitive ATP-binding of the catalytic domain of IRAK4. Although no additional information on lead optimization was provided, Galapagos says they focused their campaign on enhancing potency, selectivity, and PK properties and synthesized >1200 molecules in the process. A challenge affiliated with drugging the IRAK4 active site is the blockade of the deep pocket by Tyr262, Lys213, and Asp329, alluded to in the discovery story of [PF-06650833](#), the most advanced IRAK4 inhibitor to-date. Hence, IRAK4 inhibitors have been relatively low molecular weight compared to other kinase inhibitors, needing to achieve potency and selectivity with the limited space within the binding pocket. GLPG2534 exhibited modest selectivity over IRAK1 (28-fold, human IRAK4 IC₅₀ = 6.4 nM, human IRAK1 IC₅₀ = 179 nM). A kinase selectivity panel against 154 kinases revealed 3 hits with nanomolar potency (FLT3 IC₅₀ = 2.2 nM, FLT4/VEGFR IC₅₀ = 57 nM, TRKB IC₅₀ = 5.8 nM).



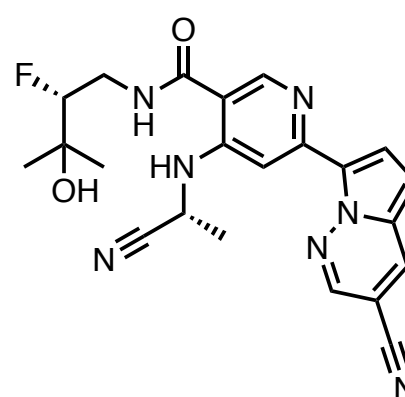
GLPG2534

Galapagos
for psoriasis & AD
(not in clinical development)



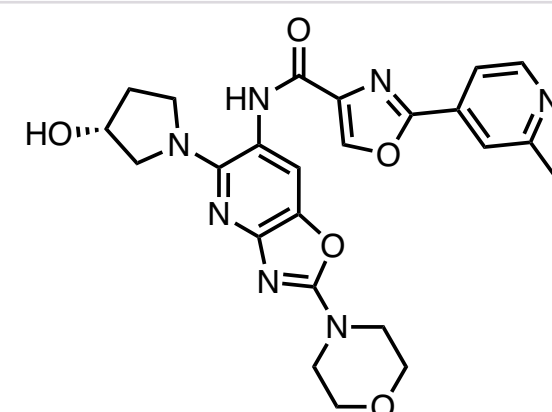
PF-06650833

Pfizer (zimlovisertib)
400 mg QD, Ph. II for RA & COVID
Ph. II for Hidradenitis
suppurativa
(discontinued)



GS-5718

Gilead (edecesertib)
≤150 mg QD, Ph. II for Lupus
Ph. II for RA & IBD
(discontinued)



CA-4948

Curis (emavusertib)
200 mg BID
Ph. Ia for r/r AML & hrMDS
(FDA partial hold Ph. Ib/Ia)

February 2023

GLPG2534

IRAK4

oral IRAK4 inhibitor

promising activity in mouse model for atopic dermatitis

HTS of kinase-focused 25K compd library vs. IRAK4 catalytic domain

Sci. Trans. Med., February 15, 2023

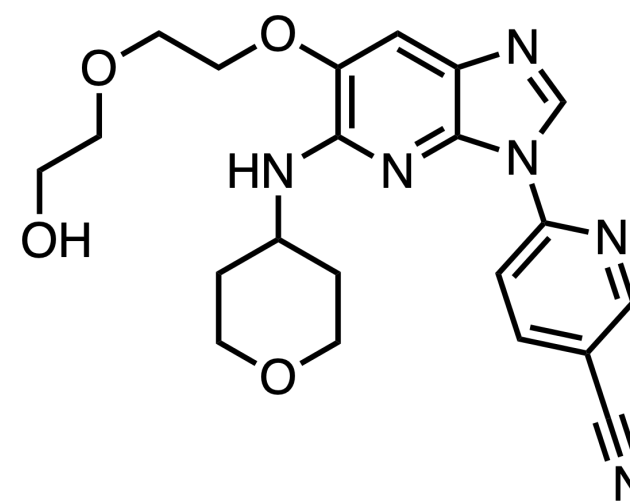
GALAPAGOS, FR + BE

paper DOI: <https://doi.org/10.1126/scitranslmed.abj3289>

[View Online](#)

Preclinical validation for skin diseases with Galapagos' clinical candidate. In an effort to understand the impact of inhibiting TLR-induced inflammatory signaling, GLPG2534 was extensively profiled in a panel of inflammatory skin disease models, in both in vivo mouse and human tissue models. Mechanistic studies revealed that inhibition of IRAK4-impacted central mediators TNF- α , IL-23, and IL-17A for psoriasis and IL-4, IL-13, and IL-33 in atopic dermatitis, by targeting T cells, keratinocytes, and granulocytes. Promisingly, GLPG2534 reduced ear thickness by 49-75% from BID doses of 3 mg/kg to 30 mg/kg, respectively, in an IL-33-induced mouse model for atopic dermatitis.

No longer in development following Pfizer's Ph. II withdrawal. Like many IRAK4 programs following Pfizer's [withdrawal](#) from the space with leading Ph. II candidate [PF-06650833](#), Galapagos seems to have discontinued work on this lead molecule which was intended for dermatology. Pfizer's PF-06650833 (zimlovisertib) has been the most advanced candidate, but was discontinued in Ph. II for Hidradenitis suppurativa most likely due to [lack of efficacy](#), but remains in the pipeline for RA and [COVID](#). Similarly, Gilead's GS-5718 (edecisertib) was withdrawn from RA and [inflammatory bowel disease](#) clinical trials, but is still being explored for [lupus](#). Within the oncology space, Curis' IRAK4 and FLT3 inhibitor, emavusertib (CA-4948), had promising single agent efficacy in [Ph. Ia](#), but continues to have a [partial hold](#) from the FDA on Ph. Ib and II expansion studies due to the observation of a patient's death due to rhabdomyolysis.



What's next? It's not clear why many companies are halting development of IRAK4 inhibitors, but [safety](#) doesn't seem to be a main concern based on various Ph. I studies. There is only one example clearly pointing to a lack of efficacy from Pfizer's Ph. II trial for Hidradenitis suppurativa. Galapagos indicated previously that it would initiate Ph. I trials since [2017](#), but active clinical trials have not been reported and GLPG2534 is not listed among its assets for [pipeline development](#). Given the tolerability and signs of human target engagement so far, Galapagos' withdrawal may be a result of the highly competitive commercial and clinical recruitment [environment](#), in which IL-17 antibodies like [dupilumab](#) are being heavily adopted and now [TYK2 inhibitors](#) seem to be on their way to blockbuster status. While there still seems to be potential for IRAK4 modulation, without clear and compelling rationale for differentiation in competitive indications, IRAK4 molecules may need to demonstrate proof-of-concept in less competitive indications first.

Patents. Galapagos holds two patents related to GLPG2534, "6-[5-amino-6-(2-ethoxyethoxy)-imidazo[4,5-b]pyridin-3-yl]-nicotinonitrile derivatives and their use as irak inhibitors" ([WO2017067848A1](#), 2017) and "Anti-inflammatory compositions comprising irak and jak inhibitors" ([WO2018149925A1](#), 2018).

February 2023

TPO473292

mGluR2/3

mGluR2/3 antagonist prodrug

Ph. II for depression

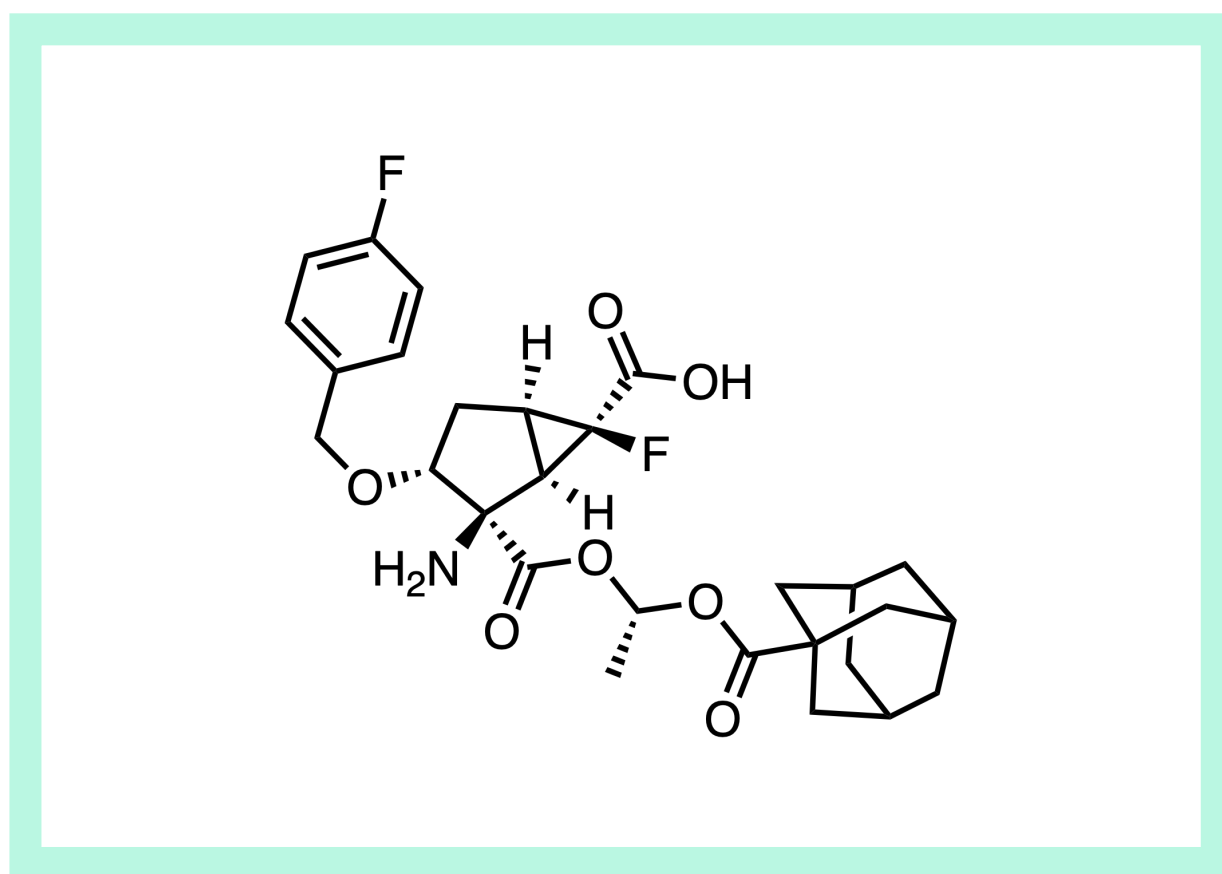
prodrug of TPO178894 (hydrophilic glutamate analog)

Drug Metab. Dispos., February 8, 2023

TAISHO PHARMACEUTICAL CO., TOKYO, JP

paper DOI: <https://doi.org/10.1124/dmd.122.001116>

[View Online](#)

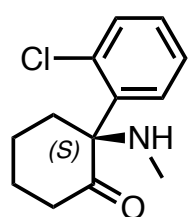


Drug Hunter Reviewer Commentary. With over two decades of experience in neuroscience drug discovery, Drug Hunter reviewer [Jake Schwarz](#) says "mGluR2/3 agonists have been explored for schizophrenia, and agonists/PAMS could be tuned to give antagonist/NAM activity, but depression is a new indication. One of the more interesting depression approaches now is the use of ketamine, an NMDA antagonist. This MoA elicits hallucinations like PCP, but dose is likely critical for the depression indication. It could be that dampening ionotropic or metabotropic glutamate receptors has a beneficial effect in patients with depression."

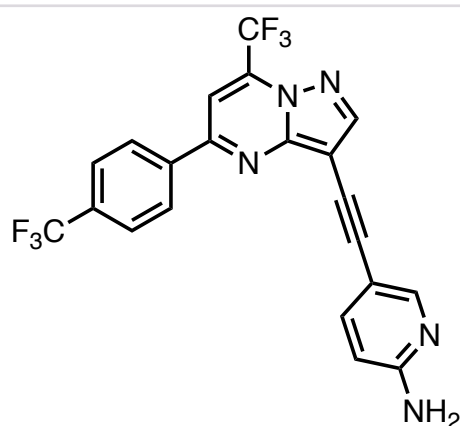
A mechanism with the antidepressant efficacy of ketamine but without the associated adverse effects? [Ketamine](#) is a molecule with a long history, starting with its initial development as an anesthetic agent with analgesic properties by Parke-Davis & Co. back in the 1950s. The (S)-(+)-enantiomer [esketamine](#) is a [non-competitive N-methyl-D-aspartate \(NMDA\) receptor antagonist](#), FDA-approved for treatment-resistant depression (TRD) in adults and known for its quick, efficacious antidepressant activity. Unfortunately, it also comes with significant adverse effects, including dissociation and hallucinations. We [recently highlighted atai Life Sciences](#) focused on developing the enantiomer, (R)-(-)-ketamine (arketamine) for TRD with the

intention of having less side effects than its isomer. SSRI/SNRIs are most widely used for the treatment of depression, the [most common psychiatric disorder worldwide](#). However, their full therapeutic effects can require several weeks/months to achieve, with about 1/3 of patients failing to respond at all. More recently, group II metabotropic glutamate 2/3 ([mGlu2/3](#)) [receptor antagonists](#) were reported to have ketamine-like antidepressant activity in rodent models, without the associated side effects, reinvigorating interest in this target.

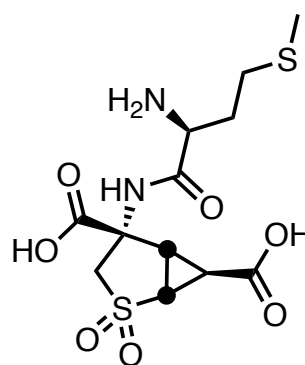
mGlu2/3 antagonism/positive allosteric modulation for the treatment of depression. These [mGlu2/3 receptors](#) localized in the cortical and limbic regions of the brain presynaptically control glutamate, the major excitatory neurotransmitter of the brain. [Several studies](#) have reported the antidepressant effects of mGlu2/3 antagonists and NAMs, as well as altered mGluR2/3 expression, in animal models for depression. Although the exact roles of these receptors remain unclear, these effects are similar to those observed for ketamine, and the underlying synaptic and neural mechanisms involved have been linked to mGluR2/3 antagonists/NAMs. The X-ray crystal structure for glutamate-derived mGluR2/3 antagonist [LY3020371](#) bound to mGlu2/3 has been reported (PDB: [5KZQ](#)).



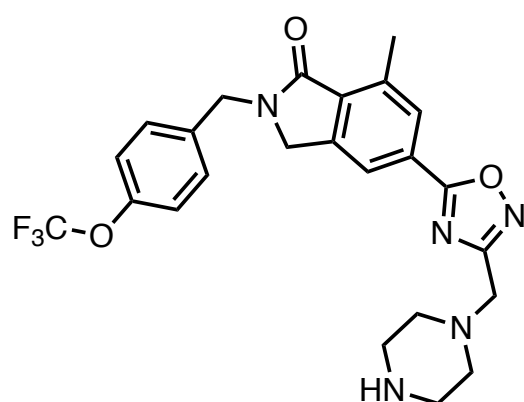
(S)-(-)-ketamine
esketamine
NMDA receptor antagonist



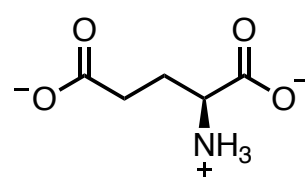
decoglurant
Ph. II mGluR2/3 NAM
for MDD



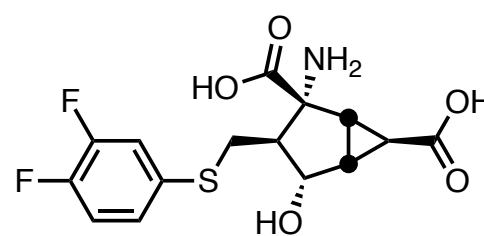
**pomaglumedad
methionil**
LY2140023
mGluR2/3 agonist for SZ



AZD8529
mGluR2/3 PAM for SZ



glutamate
neurotransmitter



LY3020371
mGluR2/3 antagonist

February 2023

TP0473292

mGluR2/3

mGluR2/3 antagonist prodrug

Ph. II for depression

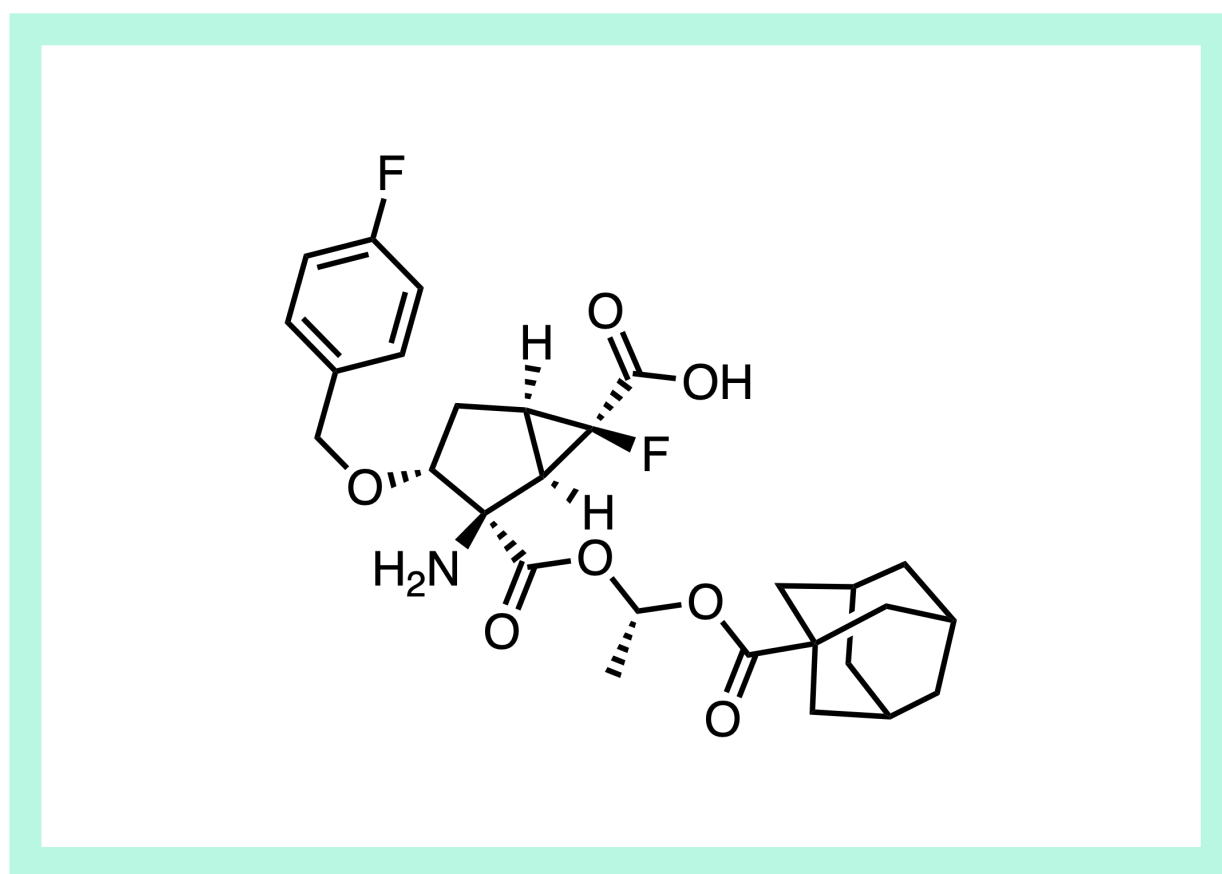
prodrug of TP0178894 (hydrophilic glutamate analog)

Drug Metab. Dispos., February 8, 2023

TAISHO PHARMACEUTICAL CO., TOKYO, JP

paper DOI: <https://doi.org/10.1124/dmd.122.001116>

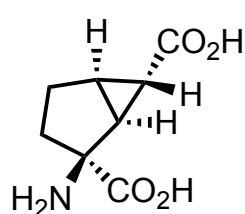
[View Online](#)



Previously explored mGluR2/3 ligands. Prior mGluR2/3 ligands have been clinically investigated for major depressive disorder (MDD) or schizophrenia (SZ), but failed to demonstrate efficacy and meet endpoints. These include the Ph. II negative allosteric modulator (NAM) for MDD, [decoglurant](#) (NCT01457677, n = 357), as well as agonist [pomaglumetad methionil](#) (LY2140023, NCT01606436) and positive allosteric modulator (PAM) [AZD8529](#) for SZ (in [several trials](#)). It has since been suggested that [selective activation of mGluR2](#) through agonists/PAMs might be a path forward for the treatment of schizophrenia.

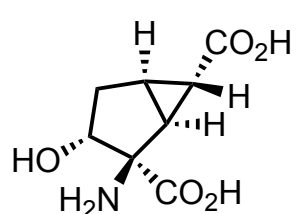
Discovery of an mGluR2/3 antagonist from a mGlu2/3 agonist via hydroxylation. [Reported in 2004](#), TP0178894 is a bicyclic glutamate derivative from a series of α -substituted ether analogs of [known mGluR2/3 agonist](#)

[compound 5](#) ([11 from 2000 JMedChem](#)). It had previously been observed that adding a [hydroxyl group to the cyclopentane ring](#) flipped the compounds from having mGluR2/3 agonist activity to antagonist activity (e.g., compound 4 [LY354740] to compound 10; 10 = [47 from 2000 JMedChem](#) [Ro 65-3479]). A similar pattern was observed in medicinal chemistry campaign that led to TP0178894, which had high affinity and antagonist activity for mGluR2 ($K_i = 2.4$ nM, $IC_{50} = 20$ nM) and mGluR3 ($K_i = 4.5$ nM, $IC_{50} = 24$ nM). Notably, substitution of the hydroxyl group for an ether provided a significant potency improvement as compared to the free -OH analog “compound 11a” (mGluR2 $K_i = 33$ nM, mGluR3 $K_i = 67$ nM), or the des-OH version (“compound 5”) with potent agonist activity. TP0178894 showed good selectivity against other mGluR subtypes and had little affinity when screened against a panel of 66 different targets (receptors, transporters, and ion channels, 10 μ M).



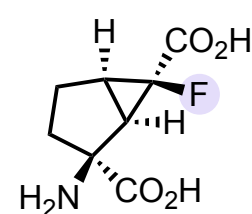
compound 4 agonist

mGluR2 $EC_{50} = 18$ nM,
 $K_i = 23$ nM
mGluR3 $EC_{50} = 63$ nM,
 $K_i = 54$ nM



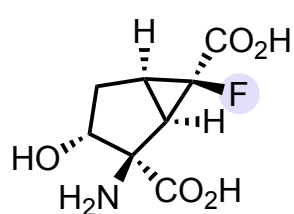
compound 10 antagonist

mGluR2 $EC_{50} > 100$ μ M,
 $IC_{50} = 36$ μ M



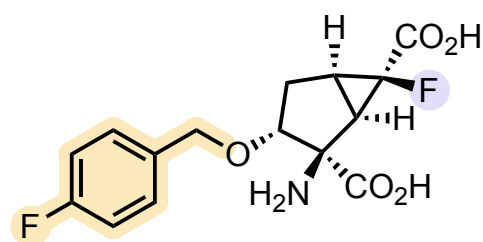
compound 5 agonist

mGluR2 $EC_{50} = 17$ nM,
 $K_i = 23$ nM
mGluR3 $EC_{50} = 81$ nM,
 $K_i = 42$ nM



compound 11a antagonist

mGluR2 $K_i = 33$ nM
mGluR3 $K_i = 67$ nM



TP0178894 antagonist

mGluR2 $K_i = 2.4$ nM,
 $IC_{50} = 20$ nM
mGluR3 $K_i = 4.5$ nM,
 $IC_{50} = 24$ nM

February 2023

TP0473292

mGluR2/3

mGluR2/3 antagonist prodrug

Ph. II for depression

prodrug of TP0178894 (hydrophilic glutamate analog)

Drug Metab. Dispos., February 8, 2023

TAISHO PHARMACEUTICAL CO., TOKYO, JP

paper DOI: <https://doi.org/10.1124/dmd.122.001116>

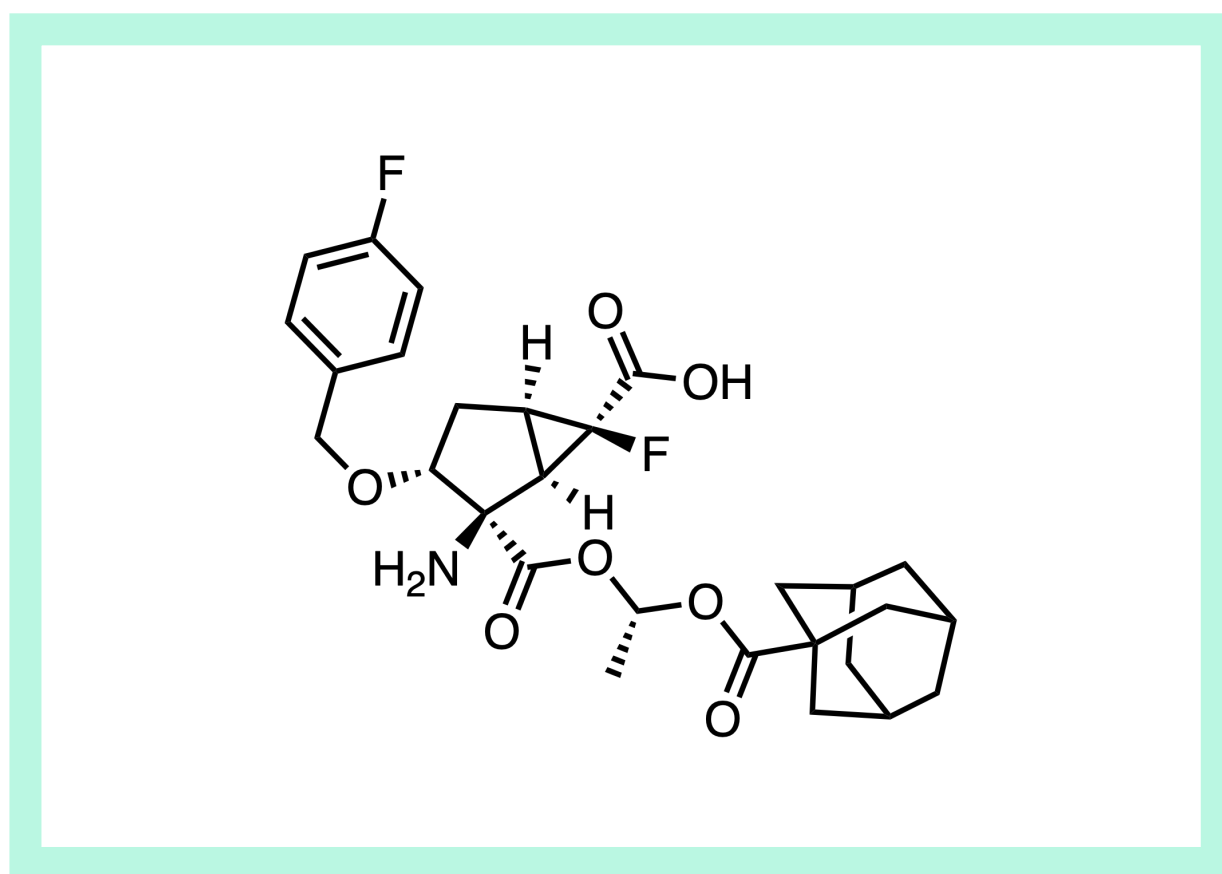
[View Online](#)

An adamantyl prodrug with 60% bioavailability of the hydrolyzed active agent in animal models. The preclinical development of TP0473292 was informed by earlier efforts with other glutamate-derived mGluR2/3 prodrugs, MGS 0210 (NCT01546051, NCT01548703) and MGS0274 (TS-134, NCT03746067, NCT03742791). The hydrophilic parent TP0178894 had a short half-life, low $V_{d_{ss}}$, low bioavailability, and a high rate of renal clearance in rats and monkeys. Luckily, an alkyl/menthol ester prodrug screen revealed the adamantane carboxylic acid (ACA) derivative to be promising.

The first adamantyl ester prodrug to enter the clinic. Adamantyl ester prodrugs have been previously used for doxorubicin and amantadine derivatives, but this is the first adamantyl ester prodrug to enter the clinic. The PK properties of prodrug TP0473292 were significantly improved over the parent, with a 10-fold increase in bioavailability and a longer half-life after oral dosing. The adamantyl acid forms a stable acylglucuronide that is cleared in the urine, suggesting limited safety concern for the byproduct.

Oral bioavailability despite metabolism by both CES1 and CES2 carboxylesterases. In addition, ester prodrug substrates are generally preferred for processing by carboxylesterase 1 (CES1) over CES2, as CES1 is the major carboxylesterase in the liver (vs. the intestines). Metabolism of a prodrug in the intestines would likely result in less systemic exposure than later metabolism in the liver, after gut absorption. While TP0473292 is a substrate for both esterases and is quickly metabolized in intestinal S9 fractions, its oral bioavailability remained surprisingly good at ~60% (r, m) even though it was more quickly hydrolyzed in rat and monkey S9 fractions than in humans. The good oral bioavailability is suggested to be due to the active compound being formed in enterocytes and permeating more extensively to the basolateral side than the luminal side by passive diffusion or active transport.

Slower elimination after oral dosing than after IV administration. Interestingly, elimination of TP0178894 in plasma after oral dosing of

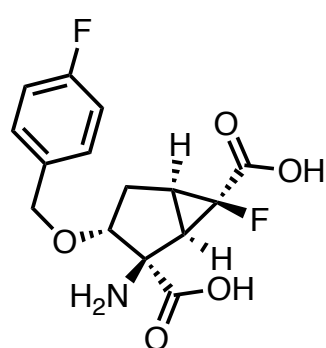


TP0473292 was slower than after IV dose of TP0178894, possibly a result of slow permeation from enterocytes into blood. It was speculated that this was not due to slow permeation from the gut lumen into enterocytes because the ACA byproduct showed a different, faster elimination profile.

Comparable efficacy to ketamine in animal models. A single dose of TP0178894 (3 mg/kg, IP) was effective in several rodent models of depression, similar to ketamine therapeutic effects, which suggests that increased synaptogenesis in the prefrontal cortex could be responsible for the rapid and sustained ketamine-like response. The TP0473292 prodrug was orally active in several animal models and reproduced similar effects observed with ketamine.

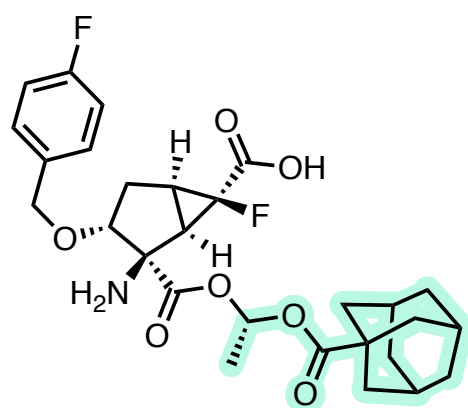
Oral PK in humans and a Ph. II study ongoing. Ph. I results for TP0473292 have been reported (NCT03919409, n = 70, completed Q1 2020). Single-ascending dose (15–400 mg) or 10-day multiple-ascending dose (50–150 mg) achieved C_{max} within 5 h in plasma and had a $t_{1/2}$ <13 h. After a single oral dose of 100 mg, the parent drug penetrated the CSF, reaching a C_{max} of 9.9 ng/mL. The human PK was similar to the preclinical studies, with C_{max} in the CSF achieved within 7 h (4 h longer than plasma), 2.2% CSF AUC compared to plasma (vs. 1.5% in rats), and a $t_{1/2}$ of 6 h. The relatively low CSF exposure was attributed to poor permeability of the active species rather than due to transporters. A Ph. II trial is currently underway for patients with treatment-resistant major depressive disorder (NCT04821271, n = 25, 50 or 100 mg QD for 3 w). With an estimated completion date of June 3, 2023, the primary outcome measure is the change from baseline on the Montgomery-Asberg Depression Rating Scale (MADRS) total score.

Patents. “Prodrug amino acid derivative” US10689327B2 (2020). “2-amino-bicyclo(3.1.0) hexane-2,6-dicarboxylic ester derivative” US8076502B2 (2010). “Method for increasing the oral bioavailability of a metabotropic glutamate 2/3 receptor antagonist” WO2014059111A2 (2014). “Novel compounds and compositions thereof for treating nervous system disorders” WO2013062680A1 (2013).



TP0178894

$t_{1/2}$ (r, m): 1.1 h, 1.8 h
 CL_{tot} (r, m): 0.53, 0.27 L/h/kg
 $V_{d_{ss}}$ (r, m): 0.47 L/kg, 0.26 L/kg
F (m): 5.8 %



TP0473292

$t_{1/2}$ (r, m): 1.4 h, 4.7 h
 CL_{tot} (r, m): 11, 2.2 L/h/kg
 $V_{d_{ss}}$ (r, m): 2.3 L/kg, 0.56 L/kg
F ('8894) (r, m): 58 %, 57 %

February 2023

M4205

KIT

selective KIT inhibitor

Ph I. for advanced GIST

HTS of ELF library (~450K cmpds) for sel. KIT(V654A)

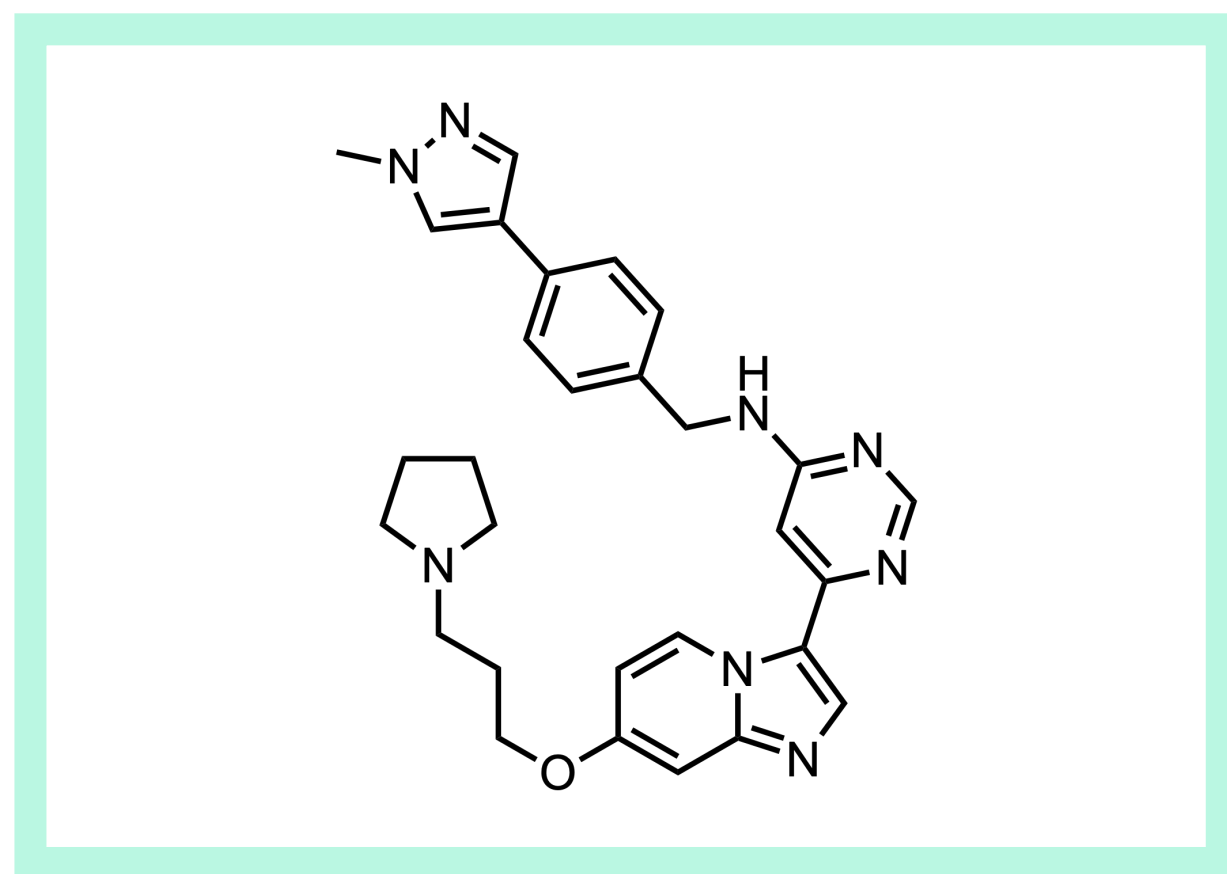
inhibition

J. Med. Chem., February 2, 2023

MERCK HEALTHCARE KGAA, DARMSTADT, DE

paper DOI: <https://doi.org/10.1021/acs.jmedchem.2c00851>

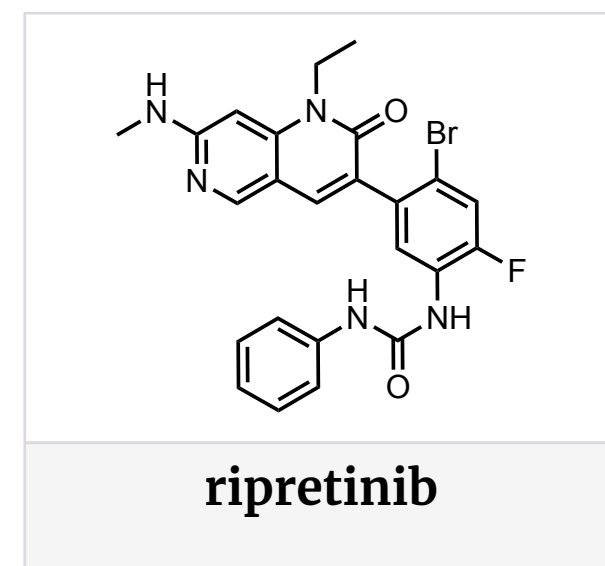
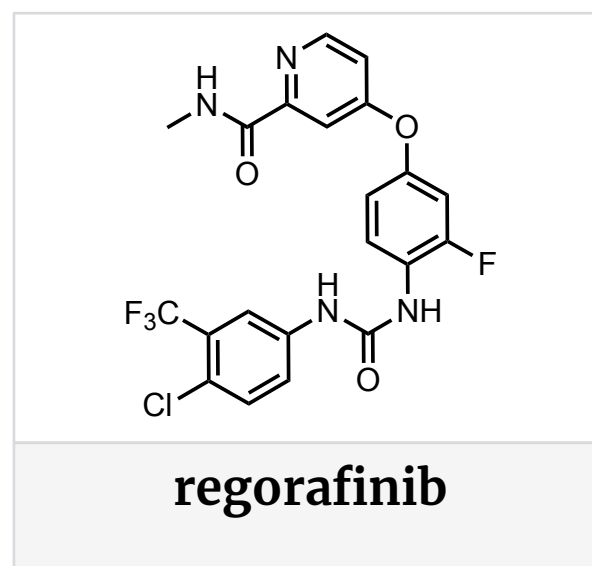
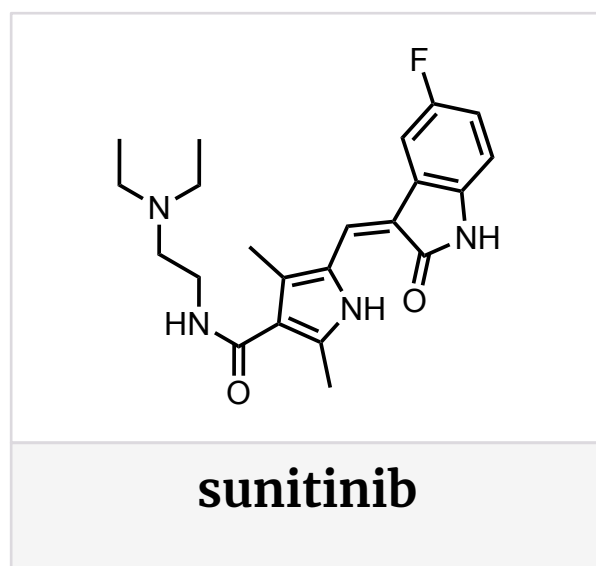
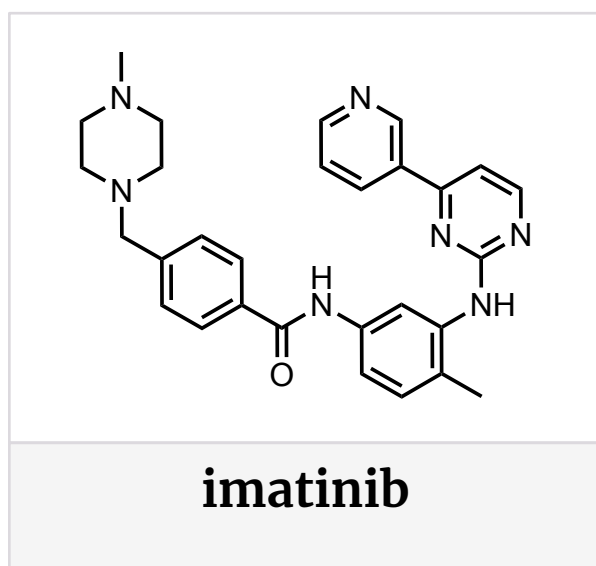
[View Online](#)



A KIT-selective, non-classical hinge binder-containing kinase inhibitor with best-in-class potential for the treatment of GIST. [M4205 \(IDRX-42\)](#) is a highly selective inhibitor of [KIT, a class III receptor tyrosine kinase](#). KIT has been difficult to target effectively due to its high propensity for both mutations in the *KIT* gene, and secondary mutations within the ATP-binding pocket leading to [5% recurrence in primary disease and up to 90% recurrence for locally advanced disease](#). The molecule is another interesting example of selectivity being achieved with non-classical [hinge binder](#) with only one strong hydrogen-bonding interaction. M4205 is currently in a Ph. I FIH trial, with the intention to [treat gastrointestinal stromal tumors \(GISTs\)](#), one of the most common mesenchymal neoplasms in the GI tract, in which 80–85% of patients have *KIT* gene mutations.

Unmet need for KIT-selective inhibitors despite several generations of molecules. KIT is [activated by stem cell factor](#) (SCF) leading to its dimerization, autophosphorylation and downstream signaling. Some tumors have deregulated KIT, leading to tumor formation and progression, while excessive KIT signaling

drives leukemia and tumors within the GI tract. Activating mutations in KIT are particularly common in GISTs, with [KIT gene mutations occurring in 80–85% of GISTs](#). KIT is susceptible to some kinase inhibitors, but lack of kinase selectivity and growing resistance of this mutation-prone target are the key challenges in this therapeutic area. The [leading first-line drug and type II kinase inhibitor, imatinib](#), has a 68% overall response rate (ORR) and median progression-free survival (PFS) of 24 months, but [secondary mutations at the ATP binding pocket](#) (or activation loop) often emerge, lowering its potency and leading to relapse. Second-line therapy is sunitinib (type I, 6% ORR, 5.6 month PDS), third-line is regorafenib (type II, 4.5% ORR, 6.3 months PDS), and fourth-line is ripretinib (type II, 9.4% ORR, 6.3 months PDS). All therapies also come with adverse effects, moderate kinase selectivity in general, and their KIT selectivity is poor - between 2.6 - 16% of kinases inhibited >80% at 1 μ M, with sunitinib being the least selective.



KIT inhibitor	imatinib	sunitinib	regorafenib	ripretinib	cmpd 1	M4205
kinase inhibitor type	type II	type I	type II	type II	type II	type II
ORR PFS (months)	68% 24	6.8% 5.6	4.5% 4.8	9.4% 6.3	--	--
kinase selectivity	2.6%	16%	4.8%	14%	7%	1.5%
KIT (V654) IC ₅₀ (nM)	720	0.8	280	31	12	44
GIST430 IC ₅₀ (nM)	59	27	131	15	--	4
GIST430/654 IC ₅₀ (nM)	4750	70	1500	185	720	48

Overall response rate (ORR), progression-free survival (PFS) in months, selectivity shown as % of kinases inhibited with >80% at 1 μ M of a panel of >395 kinases (*cmpd 1 with >30% at 1 μ M of a panel of 28 kinases), KIT (V654A): FRET-based biochemical assay with KIT V654A mutant protein, GIST430 and GIST430/654: inhibition of KIT autophosphorylation at Y703 in GIST430 cancer cell line (with activating mutation in exon 11, del560–576) and GIST430/654 (with additional imatinib resistance mutation V654A in exon 13)

February 2023

M4205

KIT

selective KIT inhibitor

Ph I. for advanced GIST

HTS of ELF library (~450K cmpds) for sel. KIT(V654A)

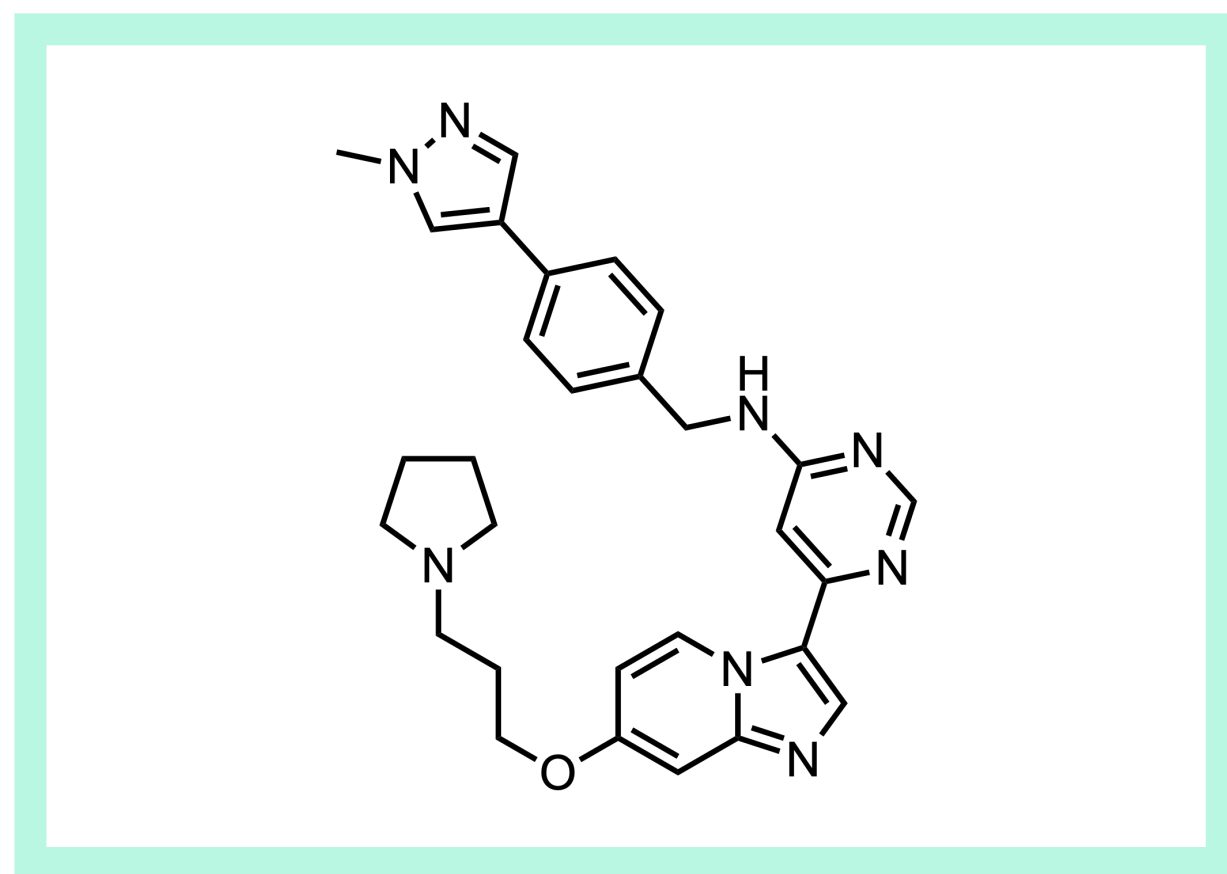
inhibition

J. Med. Chem., February 2, 2023

MERCK HEALTHCARE KGAA, DARMSTADT, DE

paper DOI: <https://doi.org/10.1021/acs.jmedchem.2c00851>

[View Online](#)



A starting point from the European Lead Factory. This campaign for a KIT-selective inhibitor began with a high-throughput screen of a [European Lead Factory \(ELF\) library](#) with an estimated ~450K compounds in a FRET-based activity assay measuring KIT(V654A) mutant inhibition. A counter-screen for inhibitors of the closely related FMS-like tyrosine kinase 3 (FLT3) was performed to get an initial read on general kinase selectivity. Ultimately, “compound 1” was identified as a starting point with 12 nM potency against the KIT(V654A) mutant and no inhibition of FLT3. In cells, it exhibited promising activity against the GIST430 cancer cell line, as well as against the imatinib-resistant GIST430/654 cell-line (V654A).

Two non-classical hinge-binding interactions and a non-amide/urea type II inhibitor. X-ray crystal structure analysis informed the lead optimization strategy, identifying the imidazopyridine nitrogen as the hinge binder with H-bonding to the hinge residue Cys673, and two non-classical C-H hydrogen bonds with other residues ([PDB: 7Zv6](#)). The benzylic substituent (pink + yellow) was shown to be deep within the pocket and a growth-vector from the imidazopyridine 6-position (mint green) was identified. It also confirmed a type II binding mode for this kinase inhibitor, with Phe811 in the DFG-out conformation, despite not having an amide or urea that is common to [type II kinase inhibitors](#).

SAR summary. Electron-donating groups at the 6-position of the imidazopyridine (mint green) improved cellular potency, while basic residues increased aqueous solubility. The nitrogen in the pyridyl unit (purple) did not engage in a polar interaction with the kinase domain of KIT, suggesting possible replacements of 2,4- or 4,6- substituted pyrimidines. The benzylic position (yellow) was identified as a site of metabolism in human and mouse liver microsomes, but this linker was determined to be particularly critical for

potency. The linker and potency could both be retained by replacing the pyridine (pink) with a benzene. The pyrrolidine (yellow) was also identified as a site for metabolism/oxidation, but was very important for potency. This was resolved by exchange for a 5-membered heterocycle, which still retained high potency. All of these changes resulted in M4205, the corresponding X-ray crystal structure of which was found to be very similar to “compound 2” with the key interactions noted in the figure above ([PDB: 7zw8](#)).

A potent and selective inhibitor with favorable CMC/ADME/PK properties and best-in-class potential. [M4205](#) demonstrated inhibitory (IC₅₀) activity in only 1.5% of the 398 kinases screened in a biochemical panel (at 1 μM), with comparable selectivity to imatinib and much better than sunitinib, regorafenib and ripretinib. Cellular activity was also assessed for 136 kinases and M4205 bound to KIT and FLT3 with 65% and 45% occupancy, respectively (NanoBRET assay, 1 μM). No safety concerns arose from a receptor panel screen against 142 safety-relevant off-target structures, and risk of cytotoxicity, neurotoxicity, genotoxicity (micronucleus, Ames tests) or DDIs were low. M4205 demonstrated high metabolic stability in liver microsomes and hepatocytes, a long half-life, good clearance across species (mouse, rat, dog and monkey) and excellent solubility (FaSSiF, FeSSiF), high permeability and low efflux. The risk of cardiac side effects was assessed to be low with human cardiomyocytes and exo vivo guinea pig papillary muscle. Interestingly, the original HTS hit, “compound 1” showed hERG channel inhibition (90% at 10 μM), so this was monitored throughout optimization. Replacing the pyridyl pyrrolidine with the aryl N-methylpyrazole the hERG liability (up to 10 μM, “compound 14”), serving as a great example of how to de-risk a molecule in development with preclinical hERG signal.

pharmacokinetics of M4205

species	mouse	rat	dog	monkey
CL (L/h/kg)	1.1	2.2	2.2	2.2
V _d (L/kg)	11.0	23.2	34.6	12.4
T _{1/2} (h) [IV]	6.9	6.8	9.6	4.4
F (%)	46	63	80	31
dose (mg/kg)	10	30	20	5

CL = (plasma clearance), V_d (volume of distribution), and T_{1/2} (half-life) were determined after single IV administration (dose: 0.2 mg/kg). F (oral bioavailability) calculated from the AUC after single admin. of dose using vehicle of suspension (mouse and rat) or solution (dog and monkey).

February 2023

M4205

KIT

selective KIT inhibitor

Ph I. for advanced GIST

HTS of ELF library (~450K cmpds) for

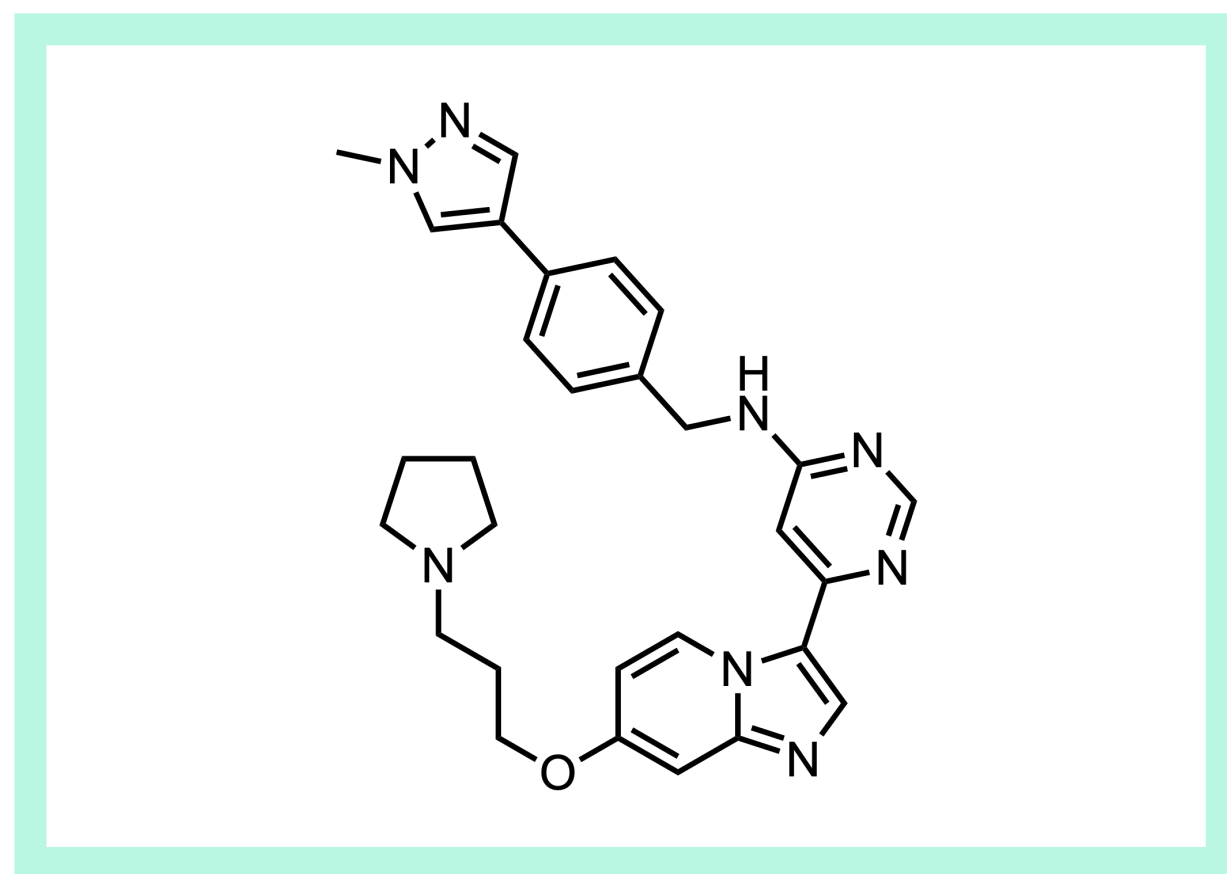
sel. KIT(V654A) inhibition

J. Med. Chem., February 2, 2023

MERCK HEALTHCARE KGAA, DARMSTADT, DE

paper DOI: <https://doi.org/10.1021/acs.jmedchem.2c00851>

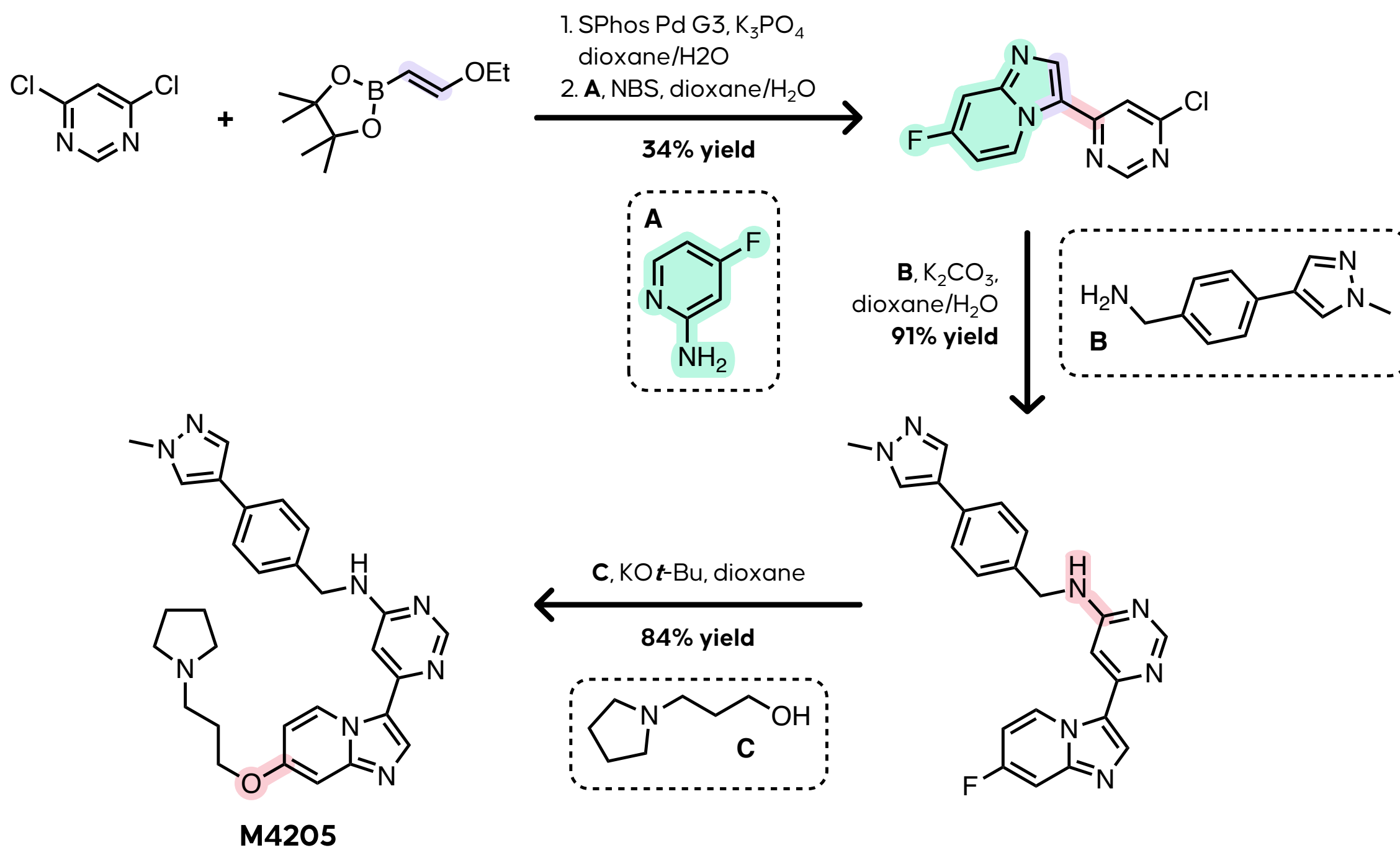
[View Online](#)



Importantly, M4205 showed high potency against KIT mutants, with IC_{50} values of 48 and 4 nM in exon 11/13- and exon 17-mutant cell lines, respectively. Corresponding effects on downstream signaling on pERK1/2 were observed, and no viability concerns up to 10 μ M were raised from the control GIST48B cell line that lacks KIT expression. Dose- and exposure-dependent in vivo tumor growth was observed, leading to regression of GIST430/654 at 35 mg/kg in rats. Further toxicology investigations in rats and dogs indicated a good risk-benefit assessment, with fewer organ effects than observed for imatinib.

Into the clinic. M4205 has progressed into Ph. I FIH clinical trials, for which they are currently recruiting ([NCT05489237](https://clinicaltrials.gov/ct2/show/study/NCT05489237)).

Synthesis Highlight. The synthetic route to M4205 and related derivatives was optimized to a convergent, four-step process that allowed rapid access to a variety of analogs during lead optimization. The initial Suzuki cross-coupling proceeded in a modest 50% yield, but installed the requisite 2 carbons primed for oxidative cyclization with NBS and aminopyridine A to form the key imidazopyridine core in 70% yield. Subsequent SNAr's with benzylic amine B and primary alcohol C proceeded in quite good yield.



February 2023

SEQ-9

Mtb 23S ribosome

oral Mtb 23S bacterial ribosome inhibitor
potent in vitro + in vivo activity against *Mycobacterium tuberculosis*

opt. of sequanamycin macrolides

Cell, February 23, 2023

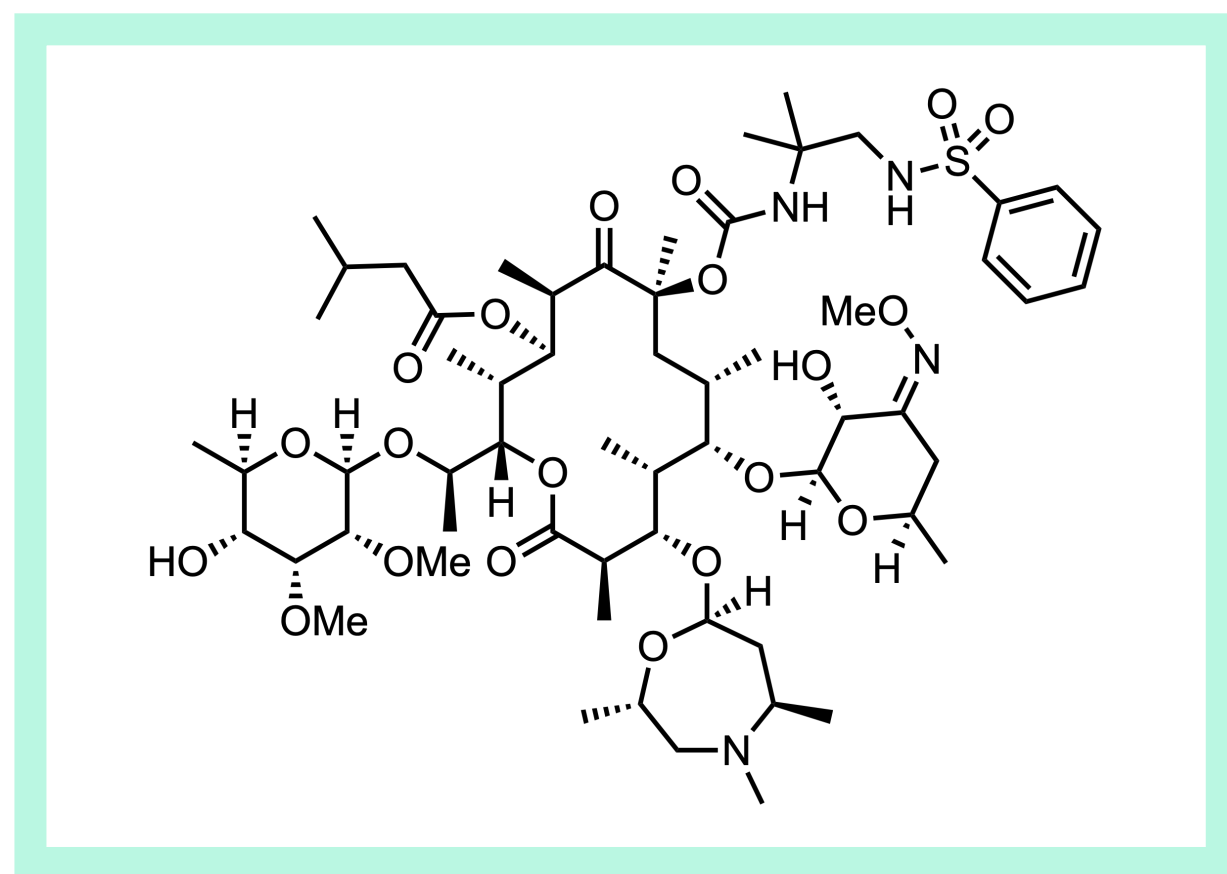
SANOFI, FR + CH

paper DOI: <https://doi.org/10.1016/j.cell.2023.01.043>

[View Online](#)

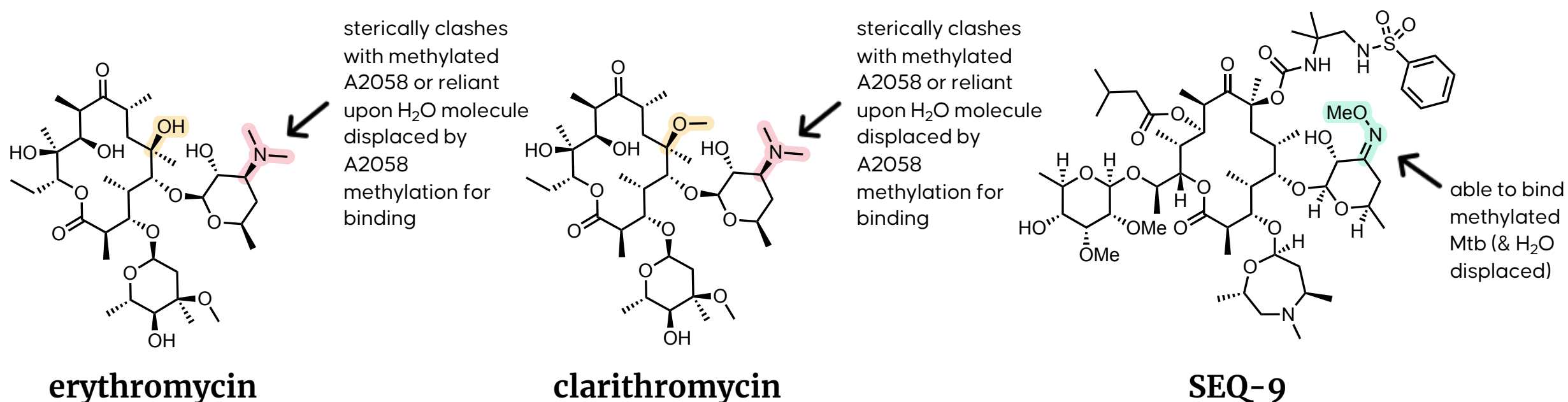
Overview. A common route of resistance to tuberculosis involves Mtb *erm37* expression, which expresses an RNA methyltransferase that methylates the A2058 position of the [23S ribosome RNA](#), hindering macrolide antibiotic binding. The sequanamycins (SEQs) are a class of molecules that overcomes this resistance mechanism, primarily attributed to the change from a dimethylamine to a carbonyl/oxime, which appears to compensate for the change in a key water molecule lacking in the mutant. Key to improving oral bioavailability and overall PK were the increase in acid and liver stability through use of an uncommon 1,4-oxazepane. The oral efficacy of the molecule is remarkable given its beyond the rule of 5 ([bRo5](#)) properties.

SEQs overcome a well-known RNA-based resistance mechanism in *Mycobacterium tuberculosis* (Mtb). The sequanamycins (SEQs), originally discovered in 1969 and produced by the bacterium *Allokutzneria albata*, are 14-membered macrolide natural products that are structurally related to the commonly-used antibacterial compounds erythromycin and clarithromycin. Generally speaking, macrolides are ineffective against *Mycobacterium tuberculosis* (Mtb) due to the [expression of the Mtb *erm37* gene](#), which encodes a methyltransferase to [methylate the RNA component of the Mtb ribosome](#). However, SEQs are able to overcome this resistance mechanism and inhibition is potent against both the native (PDB: [7SER](#)) and methylated Mtb ribosome (PDB: [7KGB](#)).



Development of SEQ-9 supports further investigation into SEQs as TB clinical candidates, with the potential for use in [new regimens](#) against drug-susceptible and drug-resistant TB.

SEQ-9 binds well despite absence of key water usually necessary for macrolide binding in the ribosome. Remarkably, the activity of the SEQs is not affected by expression of the Mtb *erm37* gene at the A2058 position on the ribosome, which inhibits the activity of both erythromycin and clarithromycin, rendering them ineffective against Mtb. This was [investigated further using cryo-EM](#), and was initially thought to be due to the multiple instances of hydrogen-bonding between the SEQ molecule and the peptide exit tunnel when compared with erythromycin and clarithromycin. Specifically, it was hypothesized that methylation of A2058 disrupts binding with erythromycin and clarithromycin, but not between SEQ and the ribosome based on potency ($IC_{50} = 0.075$ vs. $0.065 \mu\text{M}$, respectively). With erythromycin and clarithromycin, the sp^3 -hybridized dimethyl group of desosamine sterically clashes with the methylated A2058 group in the ribosome, which is absent in the SEQs (this group has been substituted for an sp^2 -hybridized oxime). However, it is more likely that the methylated A2058 plays a role in [displacing a water](#), which is key for traditional macrolide binding via their amines, but unnecessary for the oxime in SEQ-9.



February 2023

SEQ-9

Mtb 23S ribosome

oral Mtb 23S bacterial ribosome inhibitor
potent in vitro + in vivo activity against *Mycobacterium tuberculosis*

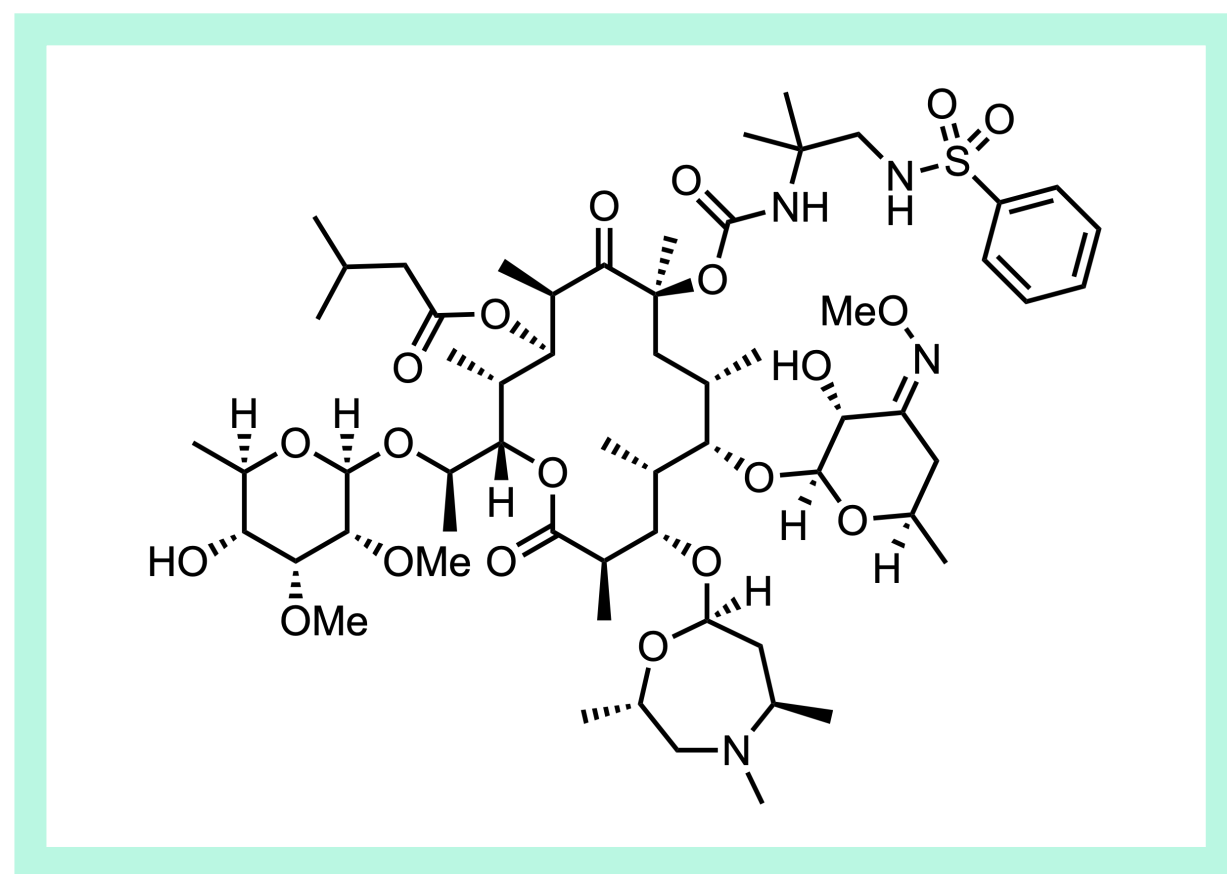
opt. of sequanamycin macrolides

Cell, February 23, 2023

SANOFI, FR + CH

paper DOI: <https://doi.org/10.1016/j.cell.2023.01.043>

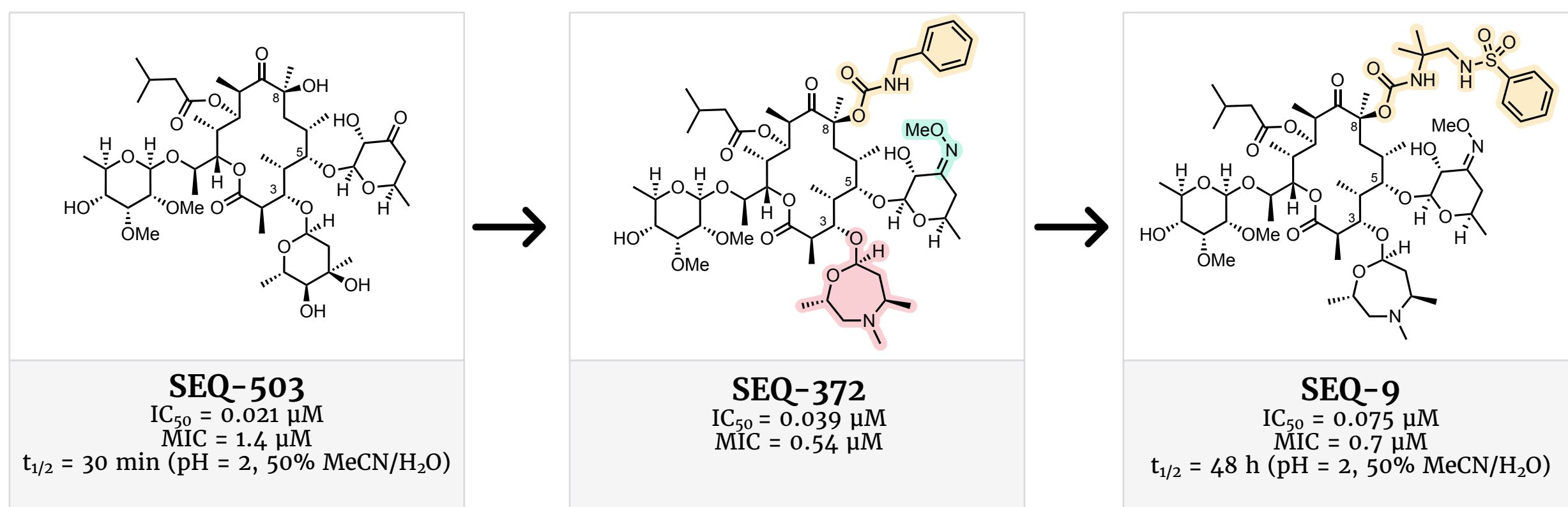
[View Online](#)



Optimization results in promising oral bioavailability and efficacy in mice. Although sequanamycin A (SEQ-503) showed promising activity against Mtb, it was inherently unstable in acidic media ($t_{1/2} = 30$ min, pH = 2, 50% MeCN/H₂O) and metabolically unstable in the liver (67% metabolized in 20 min by HLM). To improve PK properties, an unusual, 7-membered 1,4-oxazepane ring ($pK_a = 8.2$) was installed at the C-3 position, the ketone was replaced with an oxime on the C-5 sugar, and the hydroxyl was exchanged for a carbamate group at C-8. This furnished SEQ-372, which displayed dose-dependent activity in a murine model, but inhibited cytochrome 3A4 ($IC_{50} = 1.2$ μ M). Further optimization of the C-8 carbamate group resulted in SEQ-9, which exhibited excellent ADME

properties and improved $t_{1/2}$ under acidic conditions to 48 hours.

SEQ-9 was administered orally, once daily (from 37.5 to 300 mg/kg) in an acute Mtb mouse model, where the 300 mg/kg dose completely prevented bacterial growth. Mice survived at all doses compared to the control mice that died within four weeks. In a chronic Mtb model, SEQ-9 (150 mg/kg) exhibited similar efficacy to [linezolid](#) (100 mg/kg), a second-line drug for multi-resistant and extensive drug-resistant tuberculosis. This molecule serves as another interesting example of obtaining preclinical oral efficacy with bRo5 properties.



February 2023

sparsentan

ET/ATR

FIC oral, once-daily, dual ET_A/AT₁ antagonist
FDA-approved for proteinuria reduction in primary IgAN
opt. of known ET_A/AT₁ antagonist

FDA accelerated approval, February 17, 2023

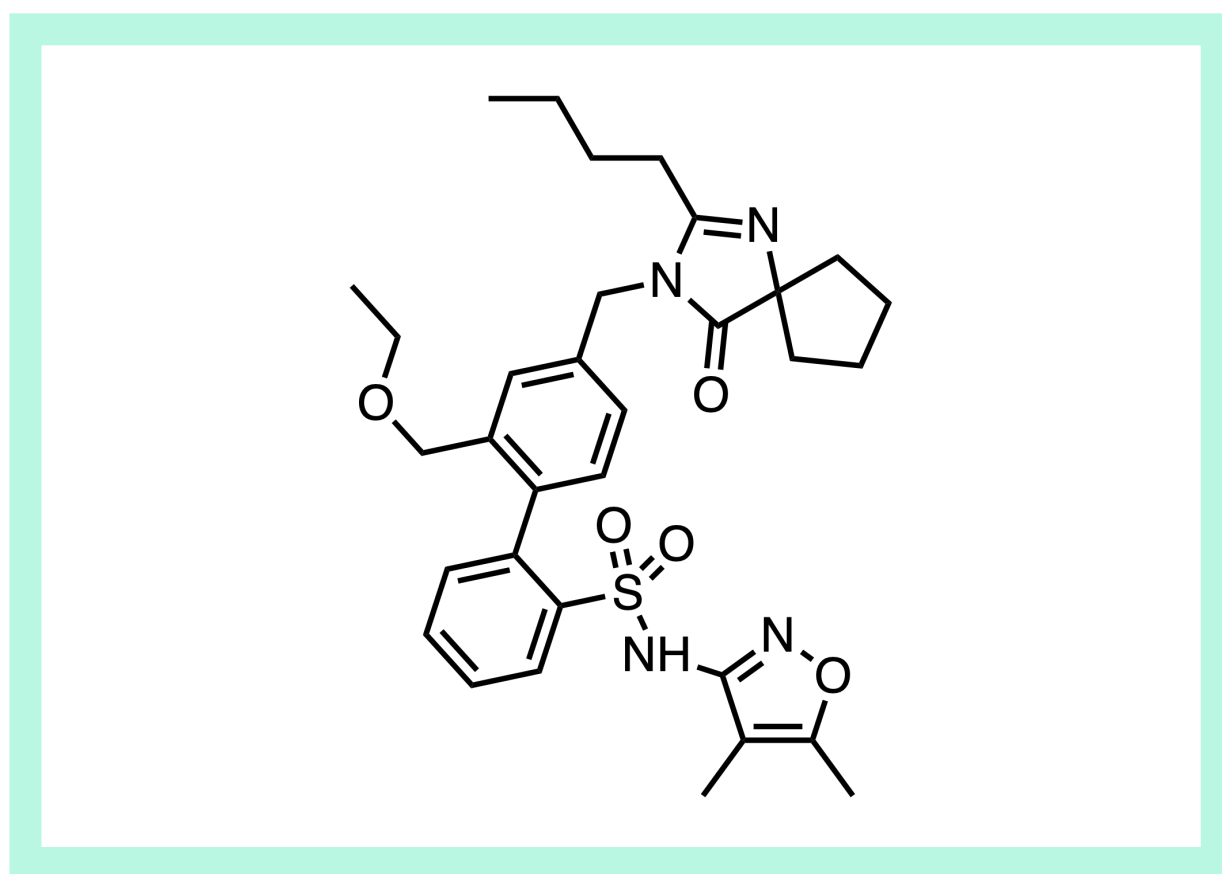
TRAVERE THERAPEUTICS, SAN DIEGO, CA

recent link: <https://ir.traverse.com/news-releases/news-release-details/traverse-therapeutics-announces-fda-accelerated-approval>

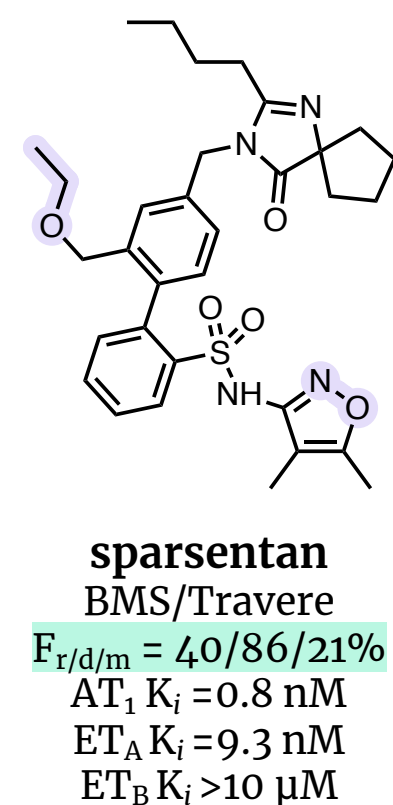
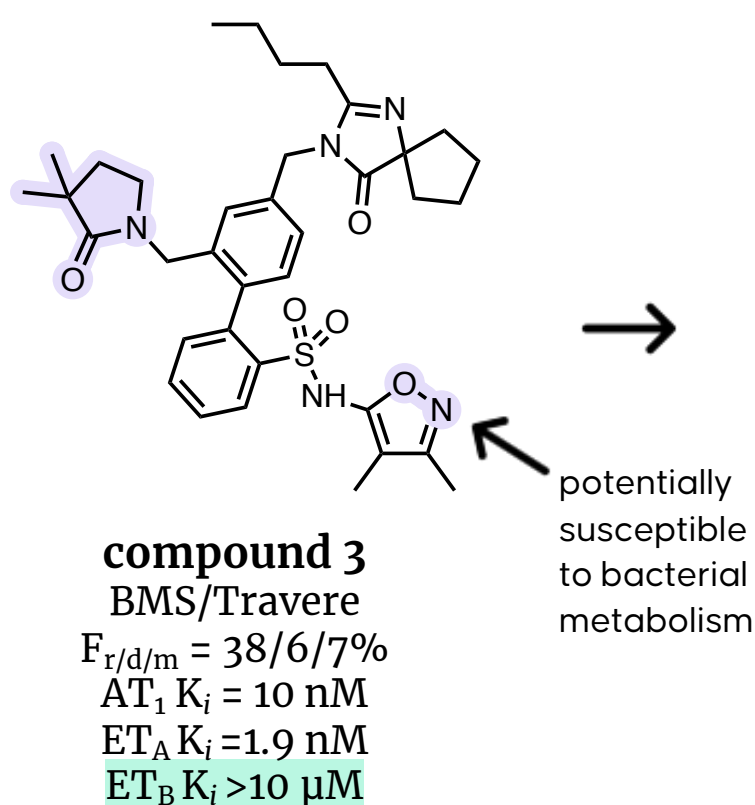
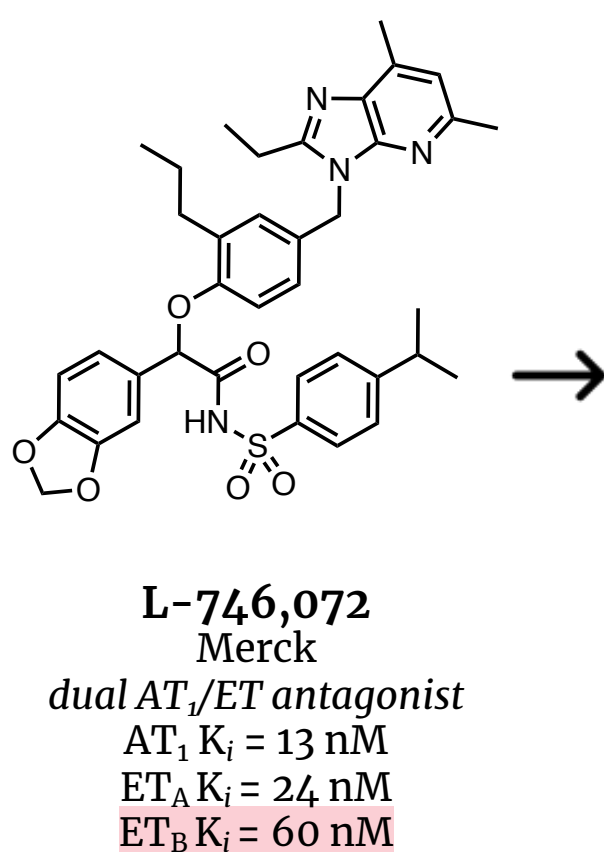
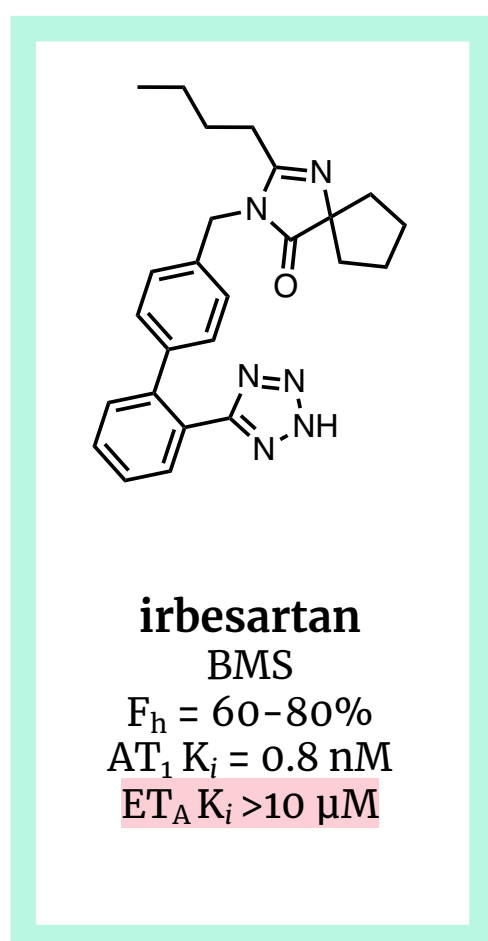
[View Online](#)

An old BMS program revitalized as a first-in-class drug in a new indication. Despite [Traverse Therapeutics](#) having a checkered industry history due to ties to Martin Shkreli, there appears to be potentially differentiating efficacy for [sparsentan's](#) ([Filspari](#)) accelerated approval thanks to its novel dual-antagonistic mechanism. It's also another example of a large pharma program (BMS346567) finding a new life in a different indication. Sparsentan's approval represents the [first non-immunosuppressive therapy](#) for IgA nephropathy (IgAN), a rare kidney disease.

A company with a checkered history, but an efficacious drug for rare kidney disease. Traverse Therapeutics was originally named Retrophin and founded in



2008 by Martin Shkreli. The company fired the CEO in 2014 after Shkreli raised the price of tiopronin by 2000%. But before completely cutting ties with Shkreli and changing their [name](#), Traverse went through a four-year string of lawsuits and counter lawsuits with the ex-CEO, eventually paying Shkreli [an undisclosed amount](#) while he was in prison serving a seven-year sentence for security fraud. The company holds the original patent for sparsentan in kidney diseases ([WO2018071784A1](#)), which it sublicensed from Ligand Pharmaceuticals in [2010](#), under the terms of potential \$15.3M in milestones and 9% net royalties in sales. Ligand acquired the license from BMS ([WO2000001389A1](#)) in 2006, which was originally focused on new targets for hypertension.



February 2023

sparsentan

ET/ATR

FIC oral, once-daily, dual ET_A/AT₁ antagonist

FDA-approved for proteinuria reduction in primary IgAN

opt. of known ET_A/AT₁ antagonist

FDA accelerated approval, February 17, 2023

TRAVERE THERAPEUTICS, SAN DIEGO, CA

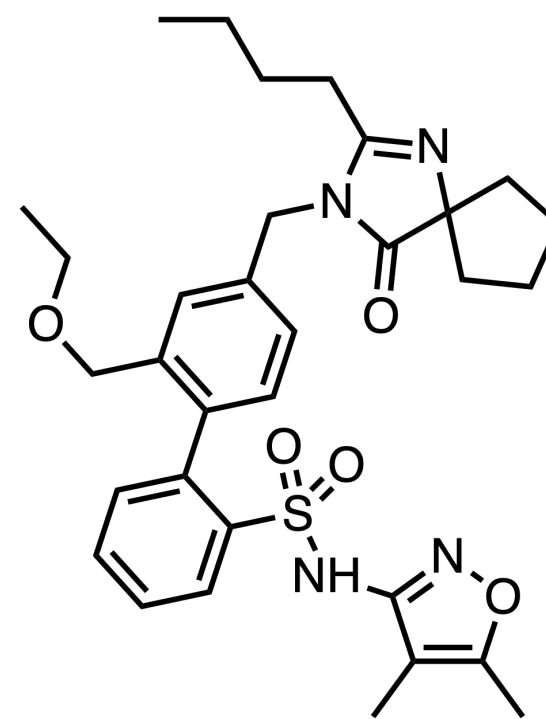
recent link: <https://ir.traverse.com/news-releases/news-release-details/traverse-therapeutics-announces-fda-accelerated-approval>

[View Online](#)

An old BMS program originally intended for hypertension. BMS originally discovered sparsentan ([BMS346567](#)) as a potential treatment for hypertension. Sparsentan is a dual antagonist for the endothelin type A (ET_A) receptor and the angiotensin II type 1 (AT₁) receptor. [ET_A and ET_B receptor substrates include endothelins \(ET-1, -2, and -3\)](#), which are homologous 21-aa peptides that influence vascular smooth muscle tone and blood flow. Activation of ET_A by ET-1 induces an intense and prolonged vasoconstriction, while activation of ET_B by any three of the ETs (at the same affinities) mediates both vaso-constriction and -dilatation, rendering ET_A selectivity important for a potential hypertension drug. The moieties of the ET substrates that most influence their binding to these receptors are the C-terminal carboxylic acid and aromatic aa's Tyr¹³ and Phe¹⁴ of the substrates; hence, ET-modulators tend to have a carboxylic acid (or isostere of) and at least several aromatic rings. ETs are some of the most potent vasoconstrictors known, but also are potent mitogens, bronchoconstrictors, and inducers of the release of other vasoactive substances. Elevated ET levels have been associated with an assortment of pathologies, rendering non-peptide ET antagonists of interest to drug discovery scientists. The structural and functional similarities between ET_A and AT₁ made them both interesting and relevant targets for the treatment of hypertension, as animal studies had shown that [simultaneous blockade of both afforded a better therapeutic effect](#).

Repositioning in IgAN. IgAN is a rare kidney disease caused by immunoglobulin A (IgA) protein buildup in the kidneys. IgA deposits degrade renal filtration mechanisms, characterized by blood in the urine (hematuria), protein in the urine (proteinuria) and a worsening loss of kidney function. High blood pressure may also be a symptom. Hypertension drugs acting on the angiotensin pathway have been used to treat nephropathies like IgAN (though not specifically approved here), and blood pressure medications of other mechanisms (e.g. [vasopressin receptor modulation](#)) have been approved for other severe kidney diseases.

Overcoming potential bacterial cleavage of an isoxazole for bioavailability. The lead optimization of sparsentan focused on improving PK properties via SAR from [compound 3](#). Compound 3 was based on a [Merck's L-746,072](#), the



studies of which indicated that the [acylsulfonamide](#) could serve as an effective [carboxylic acid isostere](#) for Ang II, the biologically activated effector molecule and peptide substrate for both AT₁ and AT₂. Merck's moderately potent dual antagonist demonstrated excellent activity, but unfortunately had low oral bioavailability (%F_{dog} = 6). Exchanging the 2'-dimethyl-pyrrolidinone for an ethoxy group improved Caco-2 permeability ~6-fold (from 30 nm/s to 170 nm/s), but oral bioavailability in monkeys remained low (%F < 5). This was suspected to be due to first-pass metabolism via [presystemic enzymatic cleavage of the 5-isoxazole ring by bacteria](#). This was addressed by employing the less susceptible 3-isoxazole regioisomer, yielding [sparsentan](#) ("compound 7") with desired oral availability (%F_{dog} = 86).

The first non-immunosuppressive therapy and only Dual Endothelin Angiotensin Receptor Antagonist (DEARA) therapy for rare kidney disease. The FDA granted accelerated approval for sparsentan based on interim results of Ph. III PROTECT study, specifically based on a 49.8% reduction in proteinuria in patients treated with the drug (200-400 mg QD) compared to 15.1% for irbesartan ([NCT03762850](#)). It remains to be seen whether or not sparsentan slows kidney function decline, but those results are expected by the end of 2023. In addition, 43% of patients exhibited complete remission of proteinuria and sustained remission for up to 4 years. Sparsentan received Orphan Drug Designation for IgAN by the FDA and EMA, and is in Ph. III for Focal Segmental Glomerulosclerosis (FSGS), which has also been granted Orphan Drug Designation in the U.S. and Europe.

An FDA-approval despite non-hERG QTc prolongation. Interestingly, QTcF prolongation was observed with sparsentan at higher doses of 800 mg (8.8 msec) and 1,600 mg (8.1 msec) but not at the prescribed doses (200-400 mg). The label says that the mechanism is unknown, but it is unlikely mediated via hERG channel inhibition. [Previous clinical studies](#) found that selective ET_A-receptor blockers caused changes in QT and QTc intervals in chronic CAD, suggesting [endothelin signaling](#) may be important to human cardiac conduction.

February 2023

daprodustat

HIF-PHD

oral, once-daily, pan-PHD inhibitor

FDA-approved for anemia in CKD patients

designed PHD 2-OG cofactor mimetic

FDA approval, February 1, 2023

GSK, PLC, LONDON, UK

recent link: <https://us.gsk.com/en-us/media/press-releases/jesduvroq-daprodustat-approved-by-us-fda-for-anemia-of-chronic-kidney-disease-in-adults-on-dialysis/>

[View Online](#)

The first and only HIF prolyl hydroxylase inhibitor approved in the US. Erythropoietin (EPO) stimulates red blood cell production (erythropoiesis). Recombinant erythropoietin (e.g. Amgen's [epoetin alfa](#)) is therefore a treatment for anemia (lack of healthy red blood cells) and was one of the first biotech products to be approved (in 1989) and subsequently [exploited by athletes like Lance Armstrong](#) as a performance-enhancing drug. Prolyl hydroxylase domains (PHDs) have been [attractive targets](#) for treating anemia, especially in chronic kidney disease (CKD) patients, as they regulate levels of hypoxia-inducible factors (HIFs) including [HIF-2](#), which induces erythropoietin production in the kidney and liver. Inhibition of PHDs prevents the proteosomal degradation of HIFs, promoting erythropoietin gene transcription among other positive effects. Daprodustat's [FDA approval](#) for anemia of CKD in adults on dialysis provides a more convenient oral alternative to injectable standard of care erythropoiesis-stimulating agents like epoetin to these patients. While daprodustat and other HIF-PHD inhibitors have been [approved internationally](#), including roxadustat (FibroGen) in China, and [vadadustat](#) (Akebia), molidustat

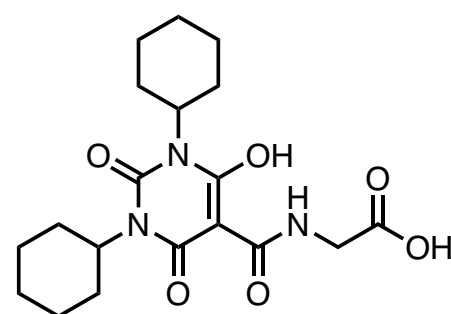
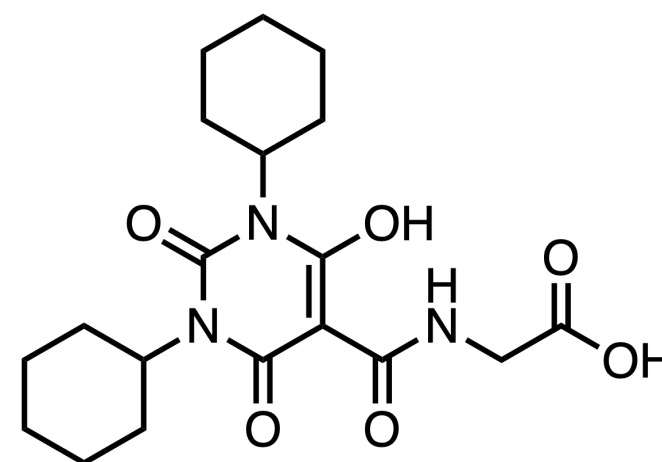
(Bayer), and enarodustat (Japan Tobacco) in Japan, daprodustat is the first to reach US approval, representing the first novel US approval for anemia in >30 years.

HIF-PHDs as targets. As the names suggest, HIF-prolyl hydroxylase domains generate hydroxylated proline-containing motifs on HIF α , recruiting the E3-ligase VHL, which mediates the proteosomal degradation of HIF. Chemists will recognize that this is the basis for [VHL-recruiting PROTACs](#), which typically contain a hydroxyproline motif. By preventing hydroxylation of HIF, and hence preventing HIF's degradation mediated by VHL, HIF-PHD inhibitors allow HIF transcription factors to sustain expression of gene products like erythropoietin. Several lines of evidence validating HIF-PHDs as targets include the observation that [HIF-2 \$\alpha\$ activating mutations](#) in humans are associated with having higher than normal levels of red blood cells, and that hematocrit increases were observed in humans with [loss-of-function mutations of one PHD2 allele](#), indicating that reduced PHD2 activity increases erythropoiesis. However, a [difficulty in drugging PHDs](#) lies in achieving selectivity over the myriad other 2-oxoglutarate (2-OG)-dependent oxygenases.

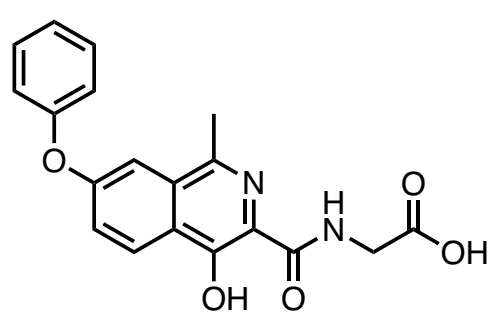
Like most HIF-PHD inhibitors, daprodustat (GSK1278863) is a mimetic of the 2-OG cofactor. Although specific details about daprodustat's discovery story are not disclosed, the lead was identified from a series of pyrimidinetrione inhibitors that tightly interacts with the catalytic iron and Arg207. Based on molecular mimicry of the five-membered chelate of natural co-factor 2-oxoglutarate (2-OG, a.k.a. alpha-ketoglutarate) and well-known inhibitor [N-oxalylglycine](#) (N-OG) in the enzyme active site, it was hypothesized that a six-membered chelate would form a stable and strong interaction and therefore result in a potent PHD inhibitor.

Relevant Co-crystal Structures. [An X-ray crystal structure](#) of a GSK1278863-related scaffold, CCT6 (PDB: [5OX5](#)) with PHD2 showed that the binding mode is related to that of the native 2-OG cofactor (PDB: [3OUJ](#)). Comparing GSK1278863 in a co-crystal structure with FIH and the orientation of CCT6 in PHD2 revealed a 20° angular difference between the pyrimidine rings, which may be due to the steric demands of the cyclohexyl rings of GSK1278863.

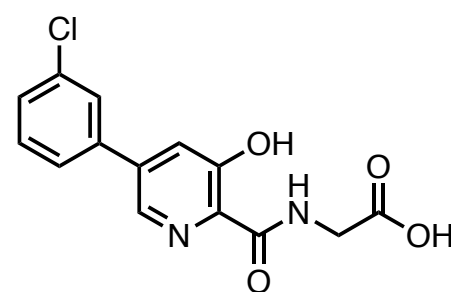
Selectivity across 2-OG-dependent enzymes evidenced by critical PHD:CP4H selectivity. While the molecule is potent (single-digit K_i) against all three HIF prolyl hydroxylase isozymes (PHD1/2/3), [GSK1278863](#) is highly selective against related 2-OG-utilizing metalloenzymes including collagen prolyl 4-hydroxylase (CP4H) and asparaginyl hydroxylase FIH. GSK1278863 is at least 1000-fold selective for PHDs compared to CP4H with IC_{50} s of 3.5–22 nM for PHD1, PHD2, and PHD3, as compared to almost 10,000 nM for FIH and >200,000 nM for CP4H. Earlier compounds had elicited undesirable cardiac valvulopathy in rodent and dog safety studies, which is suggested to be associated with off-target inhibition of CP4H.



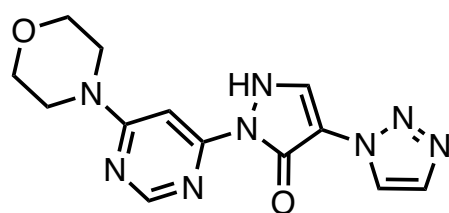
daprodustat
(GSK1278863)



roxadustat
(FBD-4592)



vadadustat
(AKB-6548)



molidustat
(BAY 85-3934)

February 2023

daprodustat

HIF-PHD

oral, once-daily, pan-PHD inhibitor

FDA-approved for anemia in CKD patients

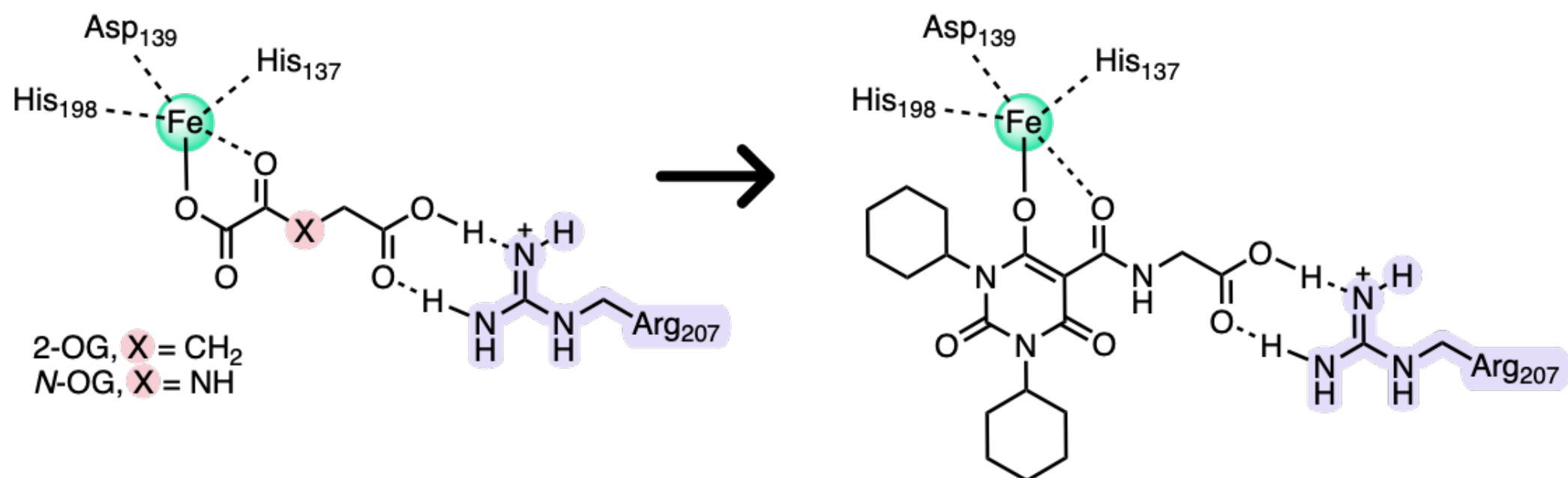
designed PHD 2-OG cofactor mimetic

FDA approval, February 1, 2023

GSK, PLC, LONDON, UK

recent link: <https://us.gsk.com/en-us/media/press-releases/jesduvroq-daprodustat-approved-by-us-fda-for-anemia-of-chronic-kidney-disease-in-adults-on-dialysis/>

[View Online](#)



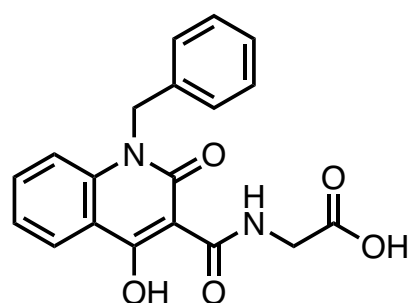
Cardiac valve lesions not observed with GSK1278863 treatment in rats or dogs.

In 14-day toxicology studies with rats and 28-day studies with mice and dogs, cardiac valve lesions were observed with compounds previously patented by GSK, including compounds A-D. Because [valvulopathies](#) have been associated with connective tissue disorders characterized by mutations in collagens and/or collagen-processing genes, inhibition of collagen prolyl 4-hydroxylase (CP4H) was hypothesized to play a role in this toxicity, despite a 20–1000-fold selectivity of compounds A-D for PHDs vs. CP4H (2.5–63K nM activity). While thromboses were observed in 3–6 month studies in rodents with GSK1278863, they were morphologically distinct from that observed with compounds A-D, and considered complications from erythrocytosis (too many red blood cells), a likely on-target effect previously observed with recombinant EPO molecules like AMG-114.

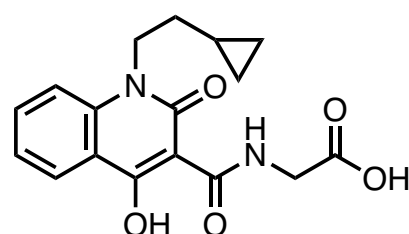
Comparable activity and safety to biologic drug epoetin alfa with a small molecule. Results from the pivotal [Ph. III trial](#) showed promise in the treatment of anemia in CKD patients: non-inferiority to epoetin alfa was demonstrated in

[mean change in hemoglobin](#) and first occurrence of MACE after a 2.5 year follow-up (25.2% daprodustat group vs. 26.7% epoetin alfa group, [NCT02879305](#)). In contrast, [vadadustat](#) previously demonstrated non-inferiority to darbepoetin alfa, but did not meet the non-inferiority criteria for major adverse cardiovascular events (MACE). Another trial ([NCT03029208](#)) corroborated its efficacy by showing that Hb concentrations and reduction in mean monthly IV iron usage was similar between the daprodustat and darbepoetin alfa groups. The [FDA approved daprodustat](#) based on the safety and efficacy data of the ASCEND-D trial, but included a boxed warning for increased risk of death, myocardial infarction, stroke, venous thromboembolism, and thrombosis of vascular access, given the related mechanism to erythropoietin-stimulating agents (ESAs). [Epoetin alfa](#) and all erythropoietin-stimulating agents in the class were all previously given [boxed warnings in 2007](#) for greater risk of death, serious cardiovascular reactions, and stroke in [CKD](#).

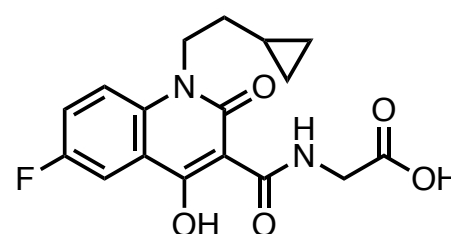
Patents. "Prolyl hydroxylase inhibitors" ([WO200715001A2](#), 2007).



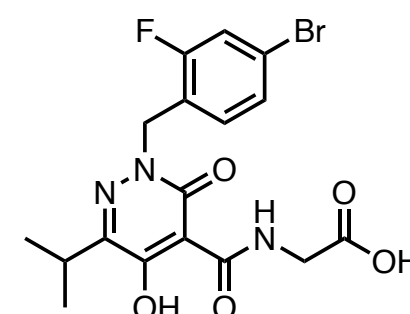
compound A



compound B



compound C



compound D

February 2023

pociredir

EED (PRC2)

oral, allosteric PRC2 inhibitor (EED)

Ph. IIb for sickle cell disease (on hold)

VLS, FBLD, de novo design + opt.

Press release, February 24, 2023

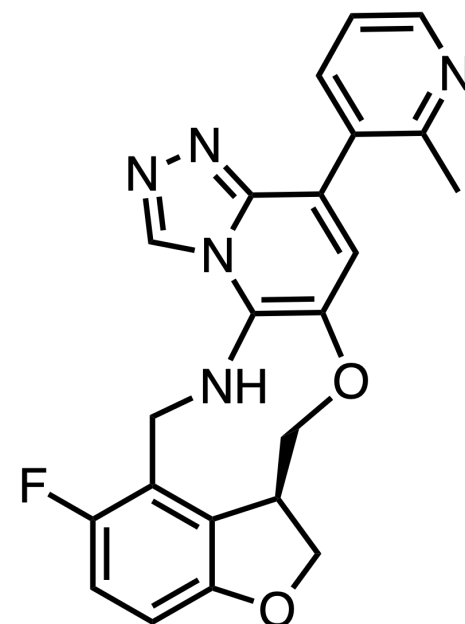
FULCRUM THERAPEUTICS, CAMBRIDGE, MA

recent link: <https://ir.fulcrumtx.com/news-releases/news-release-details/fulcrum-therapeutics-announces-clinical-hold-ftx-6058-sickle>

[View Online](#)

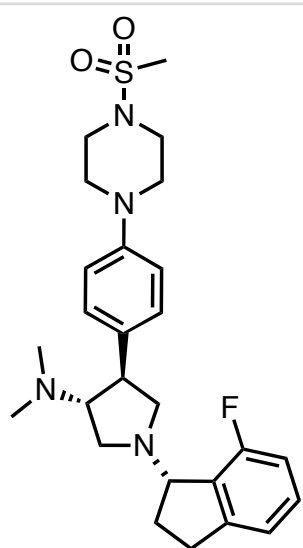
Induction of fetal hemoglobin expression by a PRC2-targeting small molecule. Pociredir (FTX-6058) is an oral, allosteric polycomb repressive complex 2 (PRC2) inhibitor that binds [embryonic ectoderm development protein \(EED\)](#) within this complex, ultimately [boosting fetal hemoglobin \(HbF\) expression](#). [Increasing HbF levels](#) has been shown to mitigate the mortality and morbidity risks of Sickle Cell Disease (SCD), which are caused by mutations in the adult hemoglobin *HBB* gene. As a small molecule treatment, this macrocyclic azolopyridine distinguishes itself in a therapeutic area [dominated by gene-correction candidates](#). For chemists, it is a notable example of a [9-membered macrocycle with relatively high ring strain](#) (~15.5 kcal/mol) that has entered clinical development.

The first clinical EED inhibitor for sickle cell disease. In recent years, EED inhibitors such as [A-395](#) have been investigated as [alternative PRC2 disruptors for targeting advanced cancers](#). The most advanced candidate is Novartis' oral, allosteric PRC2 inhibitor, [MAK683](#) (related to [EED226](#)). MAK683 is currently in Ph. I/II clinical trials for DLBCL and NPC ([NCT02900651](#)) and was highlighted as a [March '22 Molecule of the Month](#). However, FTX-6058 is the first clinical EED inhibitor for the treatment of SCD, and has [best-in-class potential](#) based on the clinically relevant HbF increases of $\leq 9.5\%$ from baseline with hemolysis and anemia improvement (6 mg QD, [NCT05169580](#)). As highlighted in our [February News Round-Up](#), it was unfortunately placed on a full clinical hold by the FDA. Regardless of where this potential SCD treatment ends up in development, it remains an interesting example of a 9-membered macrocycle with clear preclinical PD ([>80% target coverage](#)) and excellent translatability to human PK at a very low dose (≤ 10 mg).



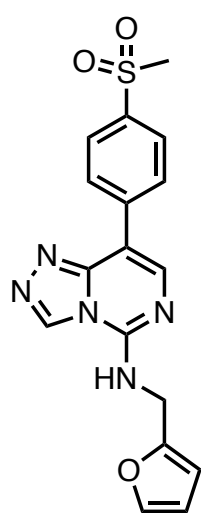
Placed on a full clinical hold due to hematological malignancy risk. FTX-6058 completed its Ph. I trial in Dec of '22 ([NCT04586985](#), n = 109), progressed into a Ph. Ib multi-center, open-label trial ([NCT05169580](#), 6 mg QD, n = 40), and was subsequently [halted](#) due to [hematological malignancies observed in preclinical studies](#). This hematological malignancy risk is not surprising given [PRC2's well-known role as a tumor suppressor](#) in certain settings. Clinical [PRC2 inhibitors with differing MOAs](#), such as [EZH2 inhibitors like tazemetostat](#), have secondary malignancies listed in their [drug label warnings](#), but the risk is more acceptable within oncology indications vs. a chronic disease like SCD that affects generally younger patients. [EZH2 also has many non-PRC2 roles in cancers](#), and the differences between EED and EZH2 inhibition remain to be fully understood. Based on the available data for PRC2 modulators, the company likely anticipated the risk of FDA action, and [plans to work with regulators to resolve the hold](#).

PRC2 as an epigenetic regulator with complicated pathobiology. The [polycomb repressive complex 2 epigenetically regulates gene expression](#) in cells by modifying chromatin structure. This histone methyltransferase (HMT) is comprised of [several subunits](#): EED, EZH2, SUZ12, and RBBP7/4; all of which are required for its methylation activity. Specifically, PRC2 influences chromatin compaction, transcription silencing, and [catalyzes the trimethylation of histone H3 at lysine 27](#) (H3K27), producing methylated products H3K27me1-3. When H3K27me3 is bound to EED, the catalytic EZH2 domain is activated and SAM-dependent methylation of neighboring histones increases. Pociredir targets the H3K27me3 recognition domain of EED, promoting methylation of H3K27 that winds up the histone complex, shuts down PRC2 complex activity, and ultimately [increases HBG1/2 gene expression, which encodes for fetal hemoglobin \(HbF\)](#). [Increasing HbF production](#) in significant enough amounts can reduce the severity of the clinical course in the anemia diseases SCD or β -thalassemia.



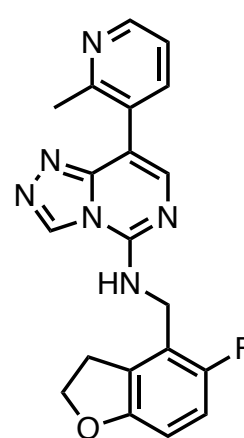
A-395

AbbVie, EED IC₅₀ = 7 nM
selective EED inhibitor



EED226

Novartis, EED IC₅₀ = 220 nM
oral EED inhibitor with
anticancer activity



MAK683

Novartis, EED IC₅₀ = 3 nM
in Ph. I/II for DLBCL + NPC

February 2023

pociredir

EED (PRC2)

oral, allosteric PRC2 inhibitor (EED)

Ph. IIb for sickle cell disease (on hold)

VLS, FBLD, de novo design + opt.

Press release, February 24, 2023

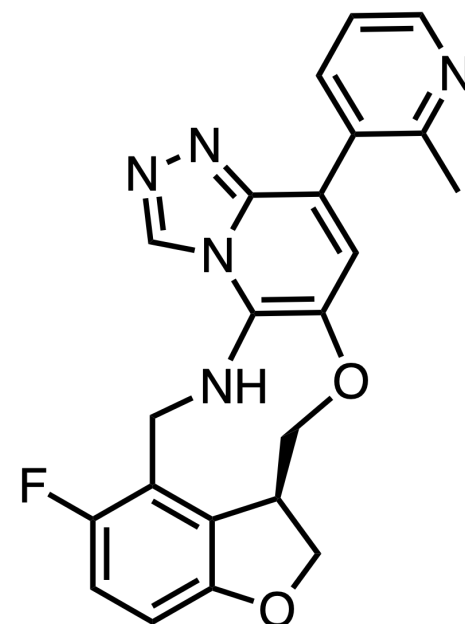
FULCRUM THERAPEUTICS, CAMBRIDGE, MA

recent link: <https://ir.fulcrumtx.com/news-releases/news-release-details/fulcrum-therapeutics-announces-clinical-hold-ftx-6058-sickle>

[View Online](#)

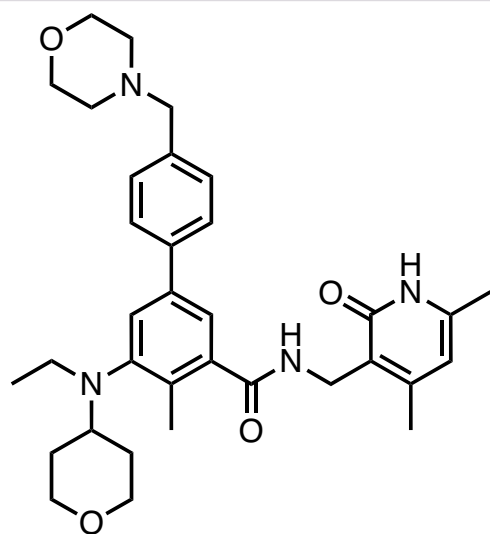
The most extensively studied PRC2 inhibitors target the more common EZH2 subunit for oncology indications. Numerous cancers have been linked to EZH2 mutations or overexpression, or other dysregulations of the PRC2 complex and/or its subunits. The first and only EZH2 (enhancer of zeste homolog 2) inhibitor to be approved was Epizyme's tazemetostat (TAZVERIK, EPZ-6438) for adv./metastatic epithelioid sarcoma and r/r follicular lymphoma (FL). This competitive EZH2 inhibitor received an FDA Fast Track designation during development for FL, for which it has an impressive 92% ORR. Other competitive EZH2 inhibitors in development for B-cell lymphomas include Ph. I/II candidates such as GSK126 (GSK2816126A, NCT02082977) and CPI-1205 (lirimetostat), but have not been progressed beyond this clinical stage. Thus, despite impressive preclinical and clinical profiles, better understanding of the unique biology of EZH2 and the PRC2 complex will be required for clinical success across indications. Secondary mutations caused by long-term administration and subsequent drug resistance have ultimately become the new challenges for unselective EZH inhibition within oncology applications that could impact development for SCD or other indications.

A literature starting point despite multiple hit generation approaches employed. Once EED was selected as a critical regulator of HbF and target of interest using CRISPR, Fulcrum's "compound screening engine," and computational data mining techniques, a full investigation into this POI and known ligands was performed. In discussing the discovery of FTX-6058, Fulcrum states that the starting point was the result of a combination of virtual screening (VLS), fragment-based drug discovery (FBDD/FBLG), de novo design, and a literature survey, each of which provided hits. A variety of synthesized analogs with various neutral core binders were utilized to map out the deep pocket and revealed a promising series of azolopyridines with single digit or subnanomolar K_d 's for EED via SPR.



Macrocyclization as a technique to optimize potency and molecular properties. Ultimately, macrocyclization was used to rigidify the molecular conformation to achieve the desired balance of potency and DMPK properties. 20 macrocyclization ideas were triaged with docking in multiple crystal structures (e.g., hydrated vs. unhydrated) and one was selected and successful, with the experimental binding mode matching the docked model closely. Fulcrum cited numerous advantages of macrocyclization, including minimization of the entropic penalty upon ligand binding, limiting potential off-target interactions by limiting possible molecule conformations, and possibly improved permeability due to reduced entropy of desolvation imposed by the preorganization of the compound. While structures were not disclosed, pairwise analysis across SPR K_D and LipE indicated that macrocyclization led to consistent affinity and compound efficiency improvements across dozens of compound pairs.

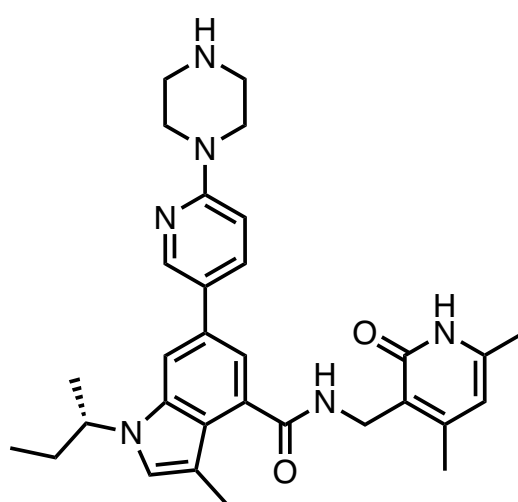
Binding within an electron-rich cage of EED. FTX-6058 binds within the H3K27me3 pocket of EED as an allosteric inhibitor of PRC2. The pocket consists of an aromatic cage of electron-rich Phe97, Tyr148, Tyr365 residues that recognize the native substrate with an electron deficient Arg at the bottom of the binding site. Most inhibitor cores are either positively-charged or neutral with electron-deficient aromatic rings. The X-ray crystal structures of EED in complex with inhibitor EED226 (PDB: 5GSA) or MAK683 are available (PDB: 7OK4).



tazemetostat

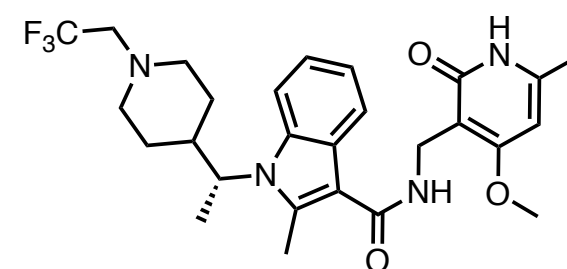
EPZ-6438, TAVERIK®

EZH2 IC_{50} = 2 nM, EZH1 IC_{50} = 392 nM
FDA-approved for adv/meta ES + r/r FL



GSK126

EZH2 IC_{50} = 9.9 nM, EZH1 IC_{50} = 680 nM
terminated Ph. I EZH2 inhibitor for DLBCL, tFL, NHL, MM or solid tumors



CPI-1205

lirimetostat, from MorphoSys
EZH2 IC_{50} = 2 nM, EZH1 IC_{50} = 52 nM
Ph. I oral EZH inhibitor

February 2023

pociredir

EED (PRC2)

oral, allosteric PRC2 inhibitor (EED)

Ph. Ib for sickle cell disease (on hold)

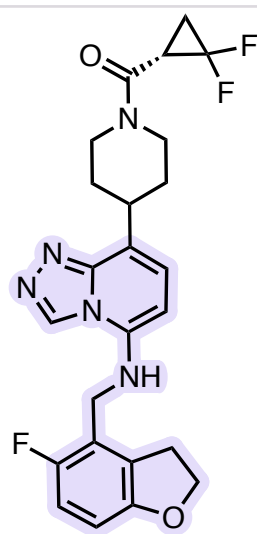
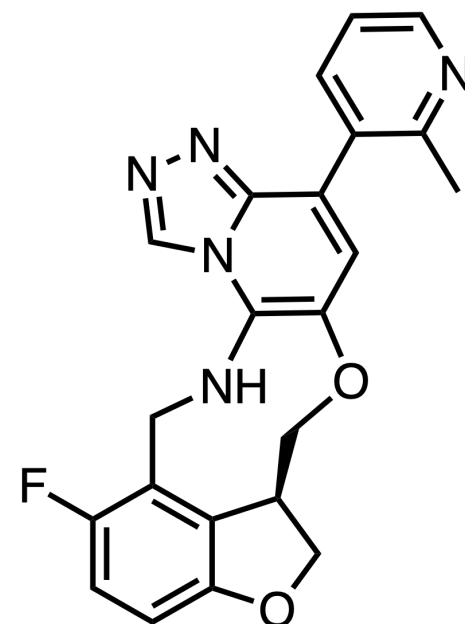
VLS, FBLD, de novo design + opt.

Press release, February 24, 2023

FULCRUM THERAPEUTICS

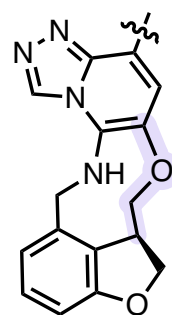
recent link: <https://ir.fulcrumtx.com/news-releases/news-release-details/fulcrum-therapeutics-announces-clinical-hold-ftx-6058-sickle>

[View Online](#)

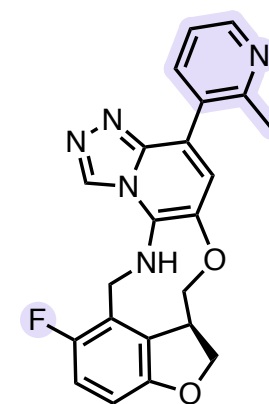


example azolopyrimidine

EED K_D (SPR) = 0.69 nM
H3K27me3 IC_{50} (P-gp HEK) = 30 nM
HLM Cl_{int} = 140 μ L/min/mg



macrocycle scaffold



pociredir (FTX-6058)

EED K_D (SPR) = 0.16 nM
H3K27me3 IC_{50} (P-gp HEK) = 12 nM
HLM Cl_{int} = 16 μ L/min/mg

In Vitro Pharmacology/Development. Final compound FTX-6058 had attractive properties across its in vitro assay cascade, including:

- EED K_D (SPR) = 0.163 nM
- PRC2 biochemical IC_{50} < 5 nM
- H3K27me3 IC_{50} (P-gp HEK cells) = 12 nM
- Primary cell activity (HbF CD34+) EC_{50} = 60 nM
- LogD (pH 7.4) = 2.6
- MDCK AB = 10.4×10^{-6} cm/s
- HLM Cl_{int} = 16.2 μ L/min/mg
- HHep Clint < 6.4 μ L/min/mill cells
- hPPB F_u = 22%
- No inhibition of 5 CYPs at 10 μ M
- MDR BA/AB = 12.4
- Mouse brain/plasma = < 0.6%
- No CYP3A4 TDI
- Not an AO substrate
- Mini-Ames and in vitro micronucleus (IVMN) negative
- hERG inhibition < 10% at 10 μ M
- Clean CEREP Safety-44 panel, KinaseProfiler panel (58 kinases), Methyltransferase panel (26 enzymes), and hepatotox. Readings (HepaRG spheroids)

FTX-6058 demonstrated robust HbF induction of 8-18% increase in hydroxyurea (HU) responsive and non-responsive CD34+ cells from healthy donors.

In Vivo Pharmacology. Significant target engagement of >50% was detected with QD dosing as low as 0.125 mg/kg in mice. FTX-6058 demonstrated dose- and time-dependent increases in both HBG1 mRNA expression and %F-cells with HbF protein levels reaching up to 40% total hemoglobin in a Townes

mouse model of SCD, (2.5 - 20 mpk, 28 d). A [2-3 fold increase of HbF relative to total Hb](#) was observed via HPLC when compared with DNMT inhibitor (5-azacytidine), G9a inhibitor (EPZ-35544), or PDE9 inhibitors (PF-04447943, IMR-687).

DMPK. The molecule is highly bioavailable across species (%F = 73 in beagles). From animal to human studies, the predicted PK properties were within 2-fold from the observed values, with the exception of $t_{1/2}$ that was 2.2x longer than predicted values.

Beagle PK - IV ROA - Dose = 0.5 mg/kg, AUC_{inf} (ng.h/mL) = 2450, C_{max} (ng/mL) = 379, T_{max} - NR, $t_{1/2}$ (h) = 5.05, Cl (mL/min/kg) = 3.41 (11.0 % HbF), V_{dss} (L/kg) = 1.30, %F = NR. **PO ROA** Dose = 1 mg/kg, AUC_{inf} (ng.h/mL) = 3591, C_{max} (ng/mL) = 413, T_{max} = 1.67, $T_{1/2}$ (h) = 5.31, Cl (mL/min/kg) = NR, V_{dss} (L/kg) = NR, %F = 73.3%.

Human PK from SAD study (2,4, 10 mg) in healthy volunteers - Dose = 10 mg, C_{max} (ng/mL) = 28.6, T_{max} (h) = 3.76, AUC (0-24, ng hr/mL) = 265, $t_{1/2}$ (hrs) = 6.72.

Successful POC in the clinic. Up until this Ph. Ib clinical hold ([NCT05169580](#)), [FTX-6058 demonstrated clinical POC](#) and achieved the increased absolute levels of HbF associated with overall patient benefit. Specifically, cohort 1 subjects (6 mg, n = 10) showed \leq 9.5% absolute HbF increases from baseline, and no difference in response to subjects on (n = 3) or off (n = 7) background hydroxyurea. Prior to trial suspension, the 12 mg dose cohort (n = 3), demonstrated \leq 10% absolute HbF increases from baseline after 42 days of treatment. And another cohort (2 mg, n = 2) demonstrated continued absolute HbF increases \leq 4.6% through the end of treatment, suggesting 2 mg as the potential minimal efficacious dose. Ultimately, FTX-6058 was generally well-tolerated in SCD patients with \leq 3 months of exposure and no serious, drug-related adverse events were reported. It had been granted FDA Fast Track and Orphan Drug designations in Dec of '22.

February 2023

pociredir

EED (PRC2)

oral, allosteric PRC2 inhibitor (EED)

Ph. IIb for sickle cell disease (on hold)

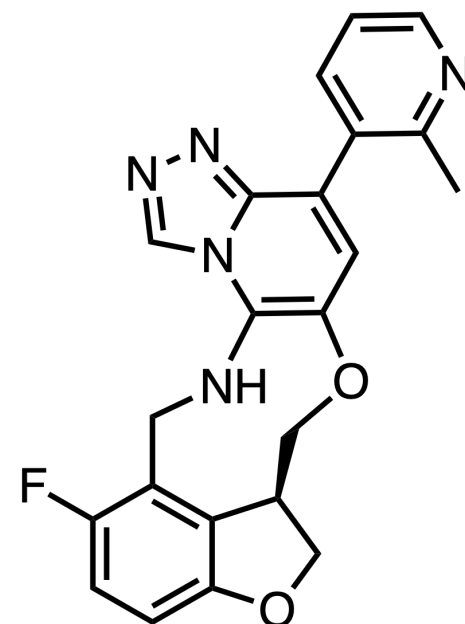
VLS, FBLD, de novo design + opt.

Press release, February 24, 2023

FULCRUM THERAPEUTICS

recent link: <https://ir.fulcrumtx.com/news-releases/news-release-details/fulcrum-therapeutics-announces-clinical-hold-ftx-6058-sickle>

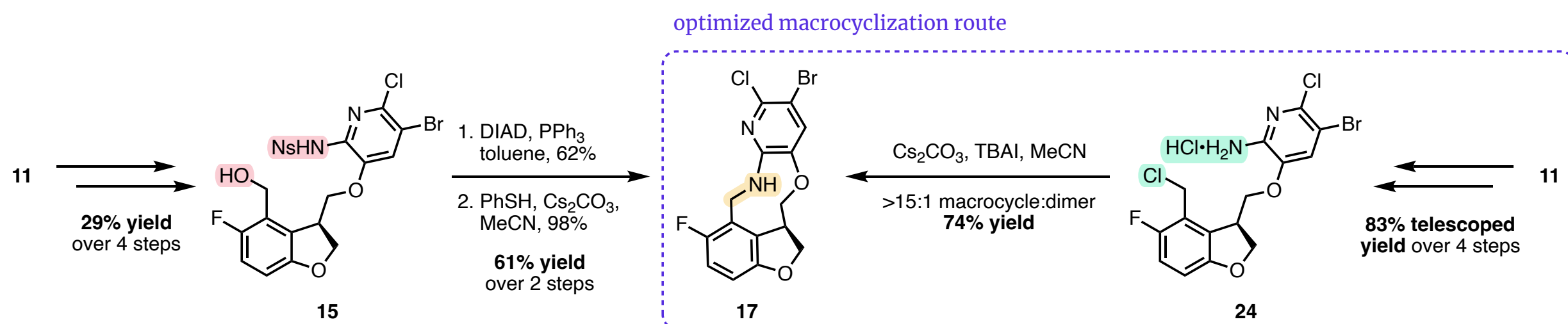
[View Online](#)



Optimization of synthesis and key macrocyclization toward FTX-6058. The initial synthesis of FTX-6058 started from advanced intermediate **11** (a 2-nitropyridine, acetal-protected aldehyde precursor to **15** and **24**) and employed a Mitsunobu macrocyclization of the benzylic alcohol and nosyl-protected amino-pyridine **15** in 62% yield. This route was modified to circumvent the aniline nosyl protection and four of the early reactions could be telescoped in an overall 83% yield, as compared to the 29% yield over 4 steps for the initial route. The new macrocyclization involved conversion of the benzylic alcohol to

chloride **24**, followed by a Finkelstein reaction, generating the benzylic iodide in situ for intramolecular displacement with the free 2-amino pyridine in 74% yield with >15:1 ratio of the desired macrocycle **17** vs. the intermolecular dimer (not shown).

Patents. "Macrocyclic azolopyridine derivatives as EED and PRC2 modulators" ([US10973805B2](#), 2020). "Macrocyclic azolopyridines" ([WO2022212746A1](#), 2022).



February 2023

QR-6401

CDK2

oral, macrocyclic CDK2 inhibitor

robust activity in ovarian cancer xenograft models

AI generative modeling + opt.

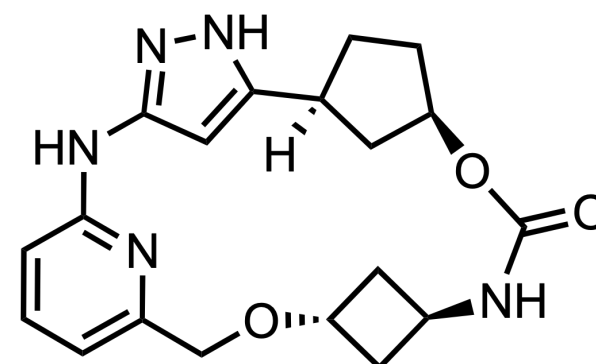
ACS Med. Chem. Lett., February 8, 2023

REGOR THERAPEUTICS GROUP, SHANGHAI, CN

paper DOI:

<https://doi.org/10.1021/acsmchemlett.2c00515>

[View Online](#)

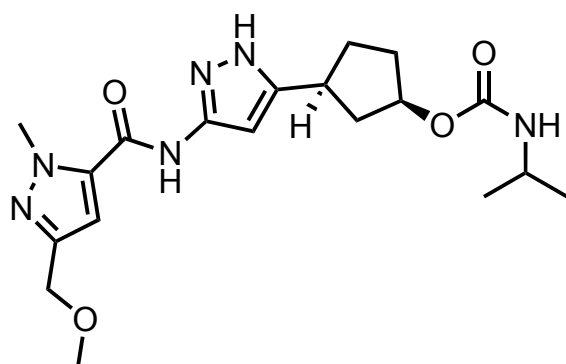


Overview. Cyclin-dependent kinase (CDK2) is a target of [recent interest](#) but selectivity has been challenging to obtain. This molecule provides an interesting example of [AI](#) being applied to lead generation. Macrocycles can be challenging to design rationally, but can lead to a variety of favorable properties (e.g. in addressing resistance or brain penetration; see article on [Turning Point](#)) and novel intellectual property space. AI could potentially assist with [identifying](#) promising starting points. While the authors admit the limitations of this approach and demonstrated superiority of human design, this case study illustrates proof-of-concept for how AI can help assist lead generation by human designers and provides a practical tool for generating viable macrocyclic starting points that could be valuable in kinase drug discovery.

The challenge of selectively targeting CDK2 against CDK family members. Thus far, inhibitors of [CDK2](#) have not been explored as extensively as against its [CDK4/6 counterparts](#). The development of selective CDK2 inhibitors could

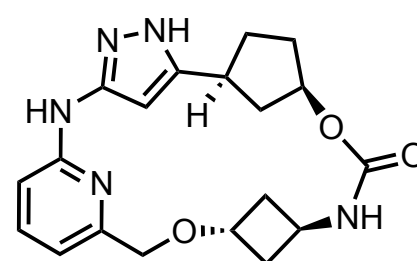
provide much needed relief for cancer patients with [drug resistance](#) to [CDK4/6 agents](#). One of the leading CDK2-selective inhibitors in the field, [disclosed at AACR in 2021](#), is [PF-07104091 \(WO2020157652A2\)](#), currently in [Ph. I clinical trials](#) as a single agent for ovarian cancer and single and combination with a CDK4 inhibitor ([PF-07220060](#)) for metastatic breast cancer.

Pursuing a validated algorithm for macrocycle lead generation. Novel acyclic starting points can be developed through [generative](#) methods employing scaffold hopping, fragment merging, fragment growing, and fragment linking methods. Macrocycles have become increasingly attractive in kinase drug discovery, as they can enable the achievement of potency, selectivity, and favorable drug-like properties by reducing the number of states a molecule can sample. One of the most well-known examples of success is the approved, differentiated macrocycle [lorlatinib](#). However, beyond [macrocyclic peptides](#), no publicly available algorithms with experimental validation are available.



PF-07104091

CDK2/cyclin E₁ K_i = 1.2 nM
CDK1/cyclin A₂ K_i = 110 nM (95x)
CDK4/cyclin D₁ K_i = 240 nM (207x)
CDK6/cyclin D₃ K_i = 470 nM (405x)
CDK9/cyclin T₁ K_i = 180 nM (155x)
GSK3β K_i = 540 nM (460x)



QR-6401

CDK2/cyclin E₁ K_i = 0.37 nM
CDK1/cyclin A₂ K_i = 22 nM (60x)
CDK4/cyclin D₁ K_i = 45 nM (122x)
CDK6/cyclin D₃ K_i = 34 nM (92x)
CDK9/cyclin T₁ K_i = 10 nM (27x)
GSK3β K_i = 5.5 nM (15x)

February 2023

QR-6401

CDK2

oral, macrocyclic CDK2 inhibitor

robust activity in ovarian cancer xenograft models

AI generative modeling + opt.

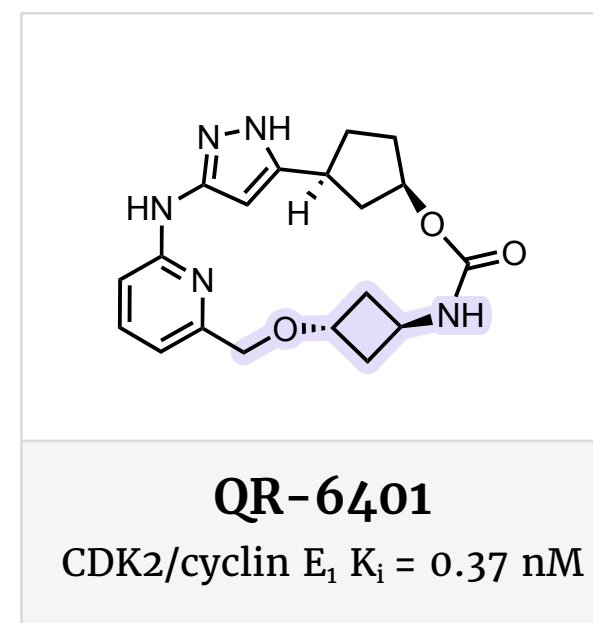
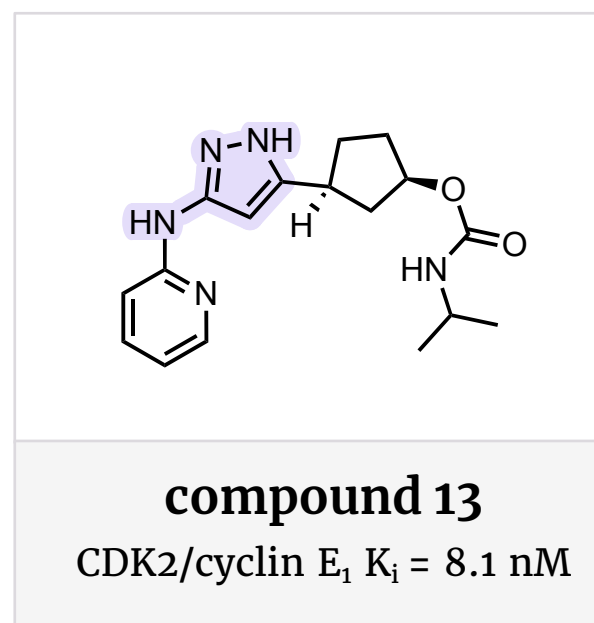
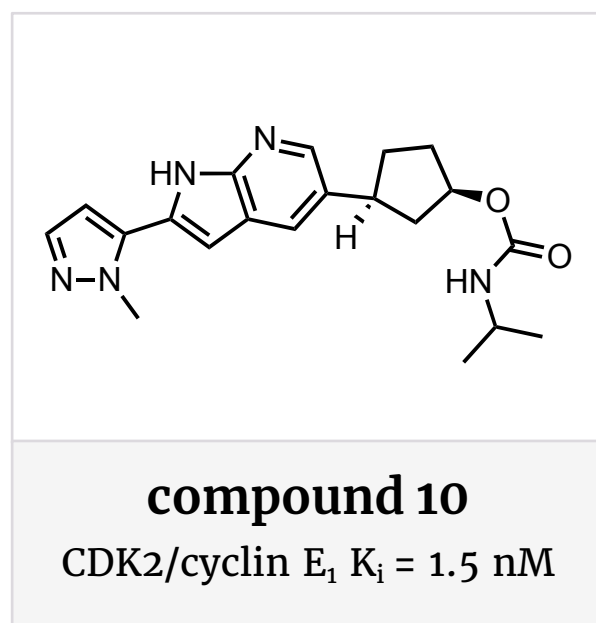
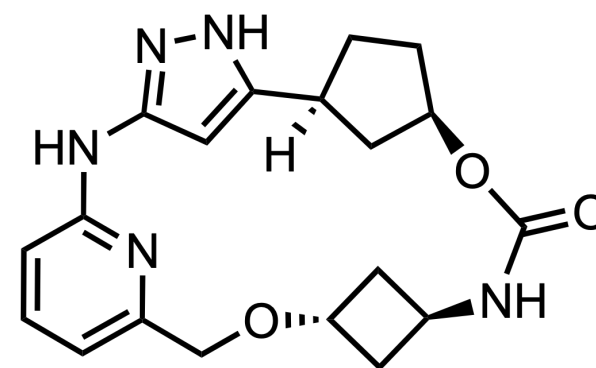
ACS Med. Chem. Lett., February 8, 2023

REGOR THERAPEUTICS GROUP, SHANGHAI, CN

paper DOI:

<https://doi.org/10.1021/acsmchemlett.2c00515>

[View Online](#)



Hinge-replacement library from a generative model. The program started from a manual selection of 10 chemotypes from disclosed CDK2-related kinase inhibitors. A Fragment-Based Variational Auto-Encoder generative model (FBVAE) was developed to perform fragment hopping by replacing the hinge binding elements of the starting compounds, producing a 3.2k molecule library, which was filtered by glide docking and visual selection to give 10 candidate starting points. Compound 10 had the most promising activity in CDK2 inhibition (CDK2/cyclin E₁ K_i = 1.5 nM) and was optimized to reduce liver clearance (data not provided). Unfortunately, selectivity for CDK1 was challenging to obtain on the compound 10 azaindole scaffold, thus other heterocyclic systems were considered. Compound 13 with an aminopyridine scaffold displayed the best selectivity of the scaffolds tested.

A three-step macrocycle generation workflow produces simple but potent analogs. Theoretical macrocycles were next generated from a linear starting point with two preferred attachment points. Linkers of preset lengths and chemotypes were then generated by a novel model called MacroTransformer. Finally, the linear starting point and linkers were connected using RDKit to form a macrocycle. Since few macrocycles exist for model training, acyclic molecules were used instead to augment the training data. A total of 7,626 macrocycles were generated from compound 13 with this approach, and filtered by docking to a total of 792 compounds of 30 clusters. Medicinal chemists then visually examined these molecules, and 10 were selected and synthesized based on feasibility. The structures of the 10 compounds shown have fairly trivial linear linkers, yet nearly all were much more potent than the acyclic starting point. An x-ray co-crystal structure of one analog (compound 19) is available (PDB: [8H6P](#)).

QR-6401 ultimately designed by humans. While the generated molecules with simple linkers were potent, they suffered from poor permeability and high efflux. Ultimately, medicinal chemists designed the interesting cyclobutyl-containing molecule, QR-6401, with acceptable intrinsic stability and good selectivity against closely related kinases. Oral administration of QR-6401 in OVCAR3 ovarian cancer xenograft mice led to significant tumor growth inhibition (TGI) of 78%.

Humans still rule. While this article claims to use AI/ML to assist with designs, the authors admit that the approach is still in its infancy. Humans were needed to triage a large set of starting points (>700) and the macrocycles generated via an algorithm had fairly trivial-looking structures. The most interesting compound reported, QR-6401, was designed by medicinal chemists. Furthermore, despite the interesting proof-of-concept, it appears that Pfizer's compound PF-07104091 is significantly more selective than QR-6401, especially on [GSK3β](#). The authors have identified an interesting and important area AI/ML may be applied to in the future, while highlighting missing areas where humans are still needed, which will serve as starting challenges for future model developers.

Past Molecules

Hall of Fame

2023

[01 January](#)

[02 February](#)

2022

[01 January](#)

[02 February](#)

[03 March](#)

[04 April](#)

[05 May](#)

[06 June](#)

[07 July](#)

[08 August](#)

[09 September](#)

[10 October](#)

[11 November](#)

[12 December](#)

2021

[01 January](#)

[02 February](#)

[03 March](#)

[04 April](#)

[05 May](#)

[06 June](#)

[07 July](#)

[08 August](#)

[09 September](#)

[10 October](#)

[11 November](#)

[12 December](#)

2020

[02 February](#)

[03 March](#)

[04 April](#)

[05 May](#)

[06 June](#)

[07 July](#)

[08 August](#)

[09 September](#)

[10 October](#)

[11 November](#)

[12 December](#)

Yearly Nominees

[2020](#)

[2021](#)

[2022](#)

Yearly Winners

[2020](#)

[2021](#)

THANK YOU!

Try Premium

and gain access to hundreds more molecule reviews like this, plus content like:

**Drug Approvals • Tech Reviews • IPO and M&As,
and more features like our sub-structure search.**

sign up for a trial today at
<https://drughunters.com/3WsorHv>

info@drughunter.com